Università degli Studi di Padova

DIPARTIMENTO DI INGEGNERIA DELL'INFORMAZIONE - DEI
Corso di Laurea in Bioingegneria

Tesi di Laurea Magistrale

Fault Detection in Type-1 Diabetic Patients Wearing a Glucose Sensor and an Insulin Pump

Relatore:
Prof. Claudio Cobelli

Correlatori:
Simone Del Favero PhD
Andrea Facchinetti PhD

Laureando:
Marco Monaro
Matricola 1020268

Anno Accademico 2013–2014

Contents

Summary

Despite the technological advance, which in the last ten years results in important enhancements of the precision and safety of the devices that make possible the realization of a wearable Artificial Pancreas (AP) for the treatment of type 1 diabetes mellitus, occasional transient failures of the continuous glucose monitoring systems - CGMs, or of the continuous subcutaneous insulin infusion systems - CSIIs, still occur during the whole day and these can lead to severe problems and risks for the safety of the patients.
In this thesis, it is developed a Fault Detection Method (FDM) like in *Facchinetti et.al* [1], where the authors advance a strategy to detect various failures of the CGMs and of the CSIIs, and to alarm when they occur.
The purpose is to extend the FDM from night to night and day, detecting both the technological failures, and the possible human errors that can easily occur during the AP utilization.
Every considered fault was simulated in many possible scenarios, so with different amplitudes, with different durations, in different point of the day and of the night and also during the events that are clearly critical for the trend of the glycemia, like the meals.
Morover, an accurate statistical analysis of the results was performed.

Chapter 1

Diabetes and DiAs Project

1.1 What diabetes is?

Diabetes is a chronic metabolic disorder in which the body cannot metabolize fats, proteins and carbohydrates because of defects in insulin secretion. It is a pathology that involves glucose regulation and can be divided in two main types: type 1, or insulin dependent, and type 2 or insulin resistant.
Nowadays, more than 370 million people in the world have diabetes and it's estimated that the number of people with this disorder will increase to 438 million by 2030, [diabetescare.net]

1.1.1 The Glycemic Control

An average meal requires approximately 4 hours for complete absorption and generally we follow a three-meal-a-day pattern so that alternate periods of plenty and fasting, [2]. To these two periods correspond: an *absorptive state* during which ingested nutrients enter the blood from gastrointestinal tract and a *post-absorptive state* during which the body's own stores must supply energy. The latter, that is needed by the cells to maintain their biological order which keeps them alive, comes from the chemical bonds in food molecules that are broken down from the body into fats, proteins and carbohydrates.
Glucose is one of the most important carbohydrates in nature and body's major energy source during the absorptive state. It's a monosaccharide, $C_6H_{12}O_6$, that is the fuel of cellular respiration: much of the absorbed glucose enters cells and is

catabolized to CO_2 and H_2O, providing energy for ATP formation. Furthermore another large fraction of it, enters into the liver cells where it occurs a net uptake of this carbohydrate that is stored as glycogen or transformed to α-glycerol phosphate and fatty acids to synthesize triglycerides, Figure 1.1.
As this period ends, synthesis of glycogen, fat, and protein ceases and catabolism[1] of all these substances begins to occur. Therefore becomes of fundamental importance that plasma glucose concentration is maintained into a normal range, about 100 mg/dL, because the brain utilizes only glucose as energy source and if the latter decreases too much several alterations of neural activity can occur.
The events that mainly maintain the right concentration during this phase are the gluconeogenesis, which consists of all the reactions that provide the formation of new glucose and the cellular utilization of fat instead of glucose to obtain energy.
The gluconeogenesis, results in the generation of glucose from his non - carbohydrate precursors such as pyruvate, lactate, glycerol and amino acids. The firsts are involved in a process called glycogenolysis that provides an amount of glucose which can supply the body's needs for several hours and other time comes from the lipolysis that results in the catabolism of triglycerides in adipose tissue yielding glycerol and fatty acids. These acids that circulate into the blood are taken up and metabolized by almost all tissues, excluding the nervous system. In particular the liver produces from these, 3 different biochemicals collectively called **ketones** or **ketone bodies**. The ketones are released into the blood and provide an important energy source during prolonged fasting.
These metabolic pathways are controlled by some endocrine factors, more precisely by two pancreatic hormones. The **pancreas** is an organ placed behind the stomach and that extends itself laterally from duodenum as shown in Figure 1.1. It mainly has exocrine function which consists in secrete digestive enzymes classified according to their target: lipases act on lipids, amylases break starches into sugars, proteases operate on proteins.
Furthermore the 1% of pancreatic cells, called isles of Langherans, has endocrine function and directly secretes three hormones into the blood: *insulin*, secreted by $\beta - cells$, which removes glucose from blood and promotes his entrance into the cells, *glucagon*, secreted by $\alpha - cells$, which releases glucose from depositis of glycogen

[1]Set of degradative chemical reactions that breaks down complex molecules into smaller units to release energy.

into the blood, *somatostatin*, secreted by $\delta - cells$, which inhibits the secretion of both insulin and glucagon.

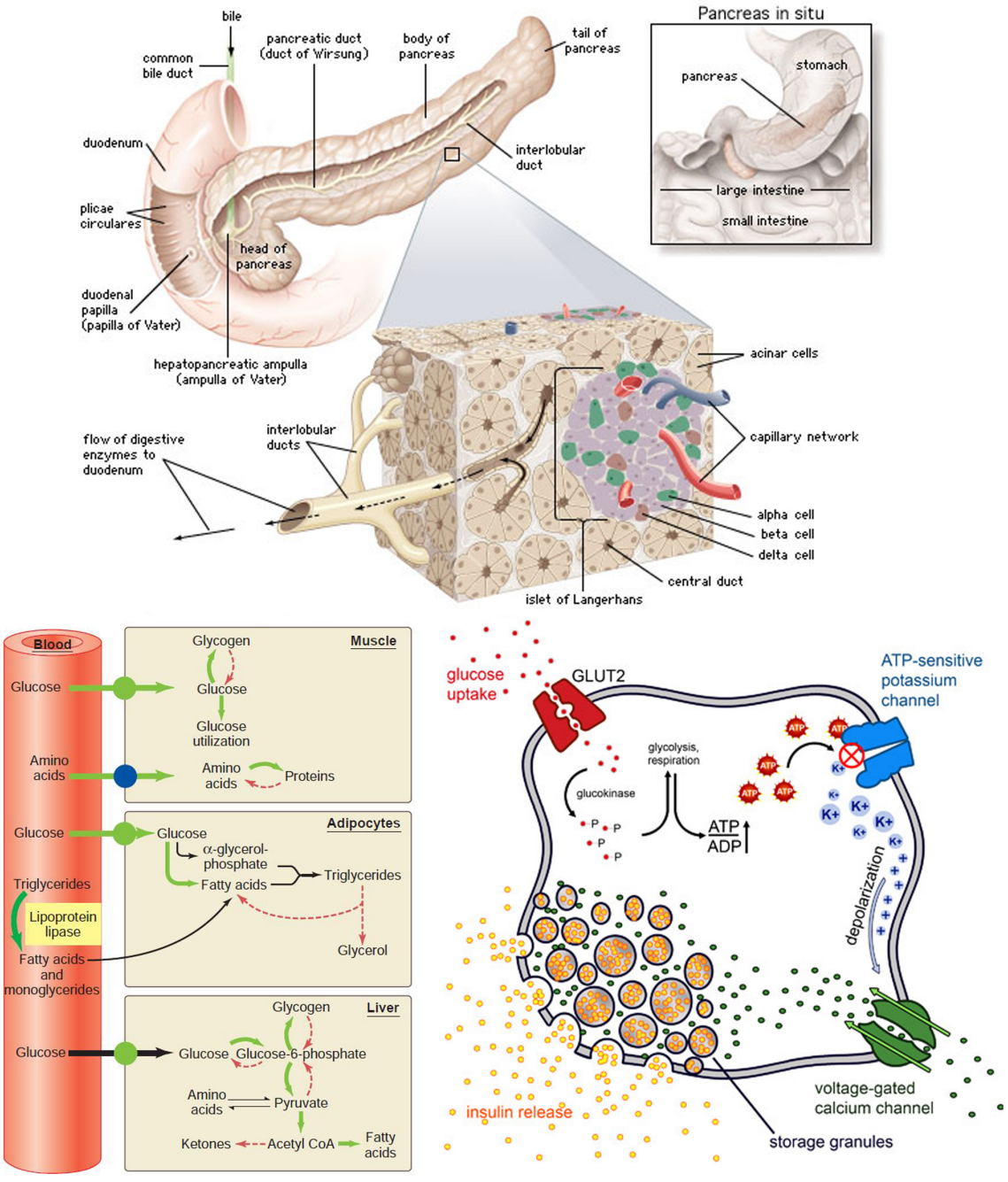

Figure 1.1: Plasma Glucose and Insulin Secretion.

Insulin is the most important controller of organic metabolism [2]. As shown in Figure 1.1, it induces its effects by binding to specific receptors on the plasma membranes of its target cells and so triggers signal transduction pathways that influence the plasma membrane transport proteins of the target cell.
If plasma glucose concentration increases, the $\beta - cells$ are activated and start the secretion of insulin which induces cytoplasmic vesicles that contain a glucose transporter, called $GLUT - \bullet$ depending by the cell target, merge themselves with the plasma membrane and this results in a greater rate of glucose movement from the extracellular fluid into the cells.
Stimulation and activation of pancreatic $\beta - cells$ cells depends on changes in plasma glucose concentration.

1.1.2 Type I Diabetes

Normally the body can balance the amount of insulin and glucose and thus regulate the levels of the latter that typically are: fasting (before eating) $(70 - 99) mg/dl$ and $140 mg/dl$ or less two hours after a meal.
The complex regulation of blood glucose is not successful in diabetes, in particular in the Type 1 that is an autoimmune condition, due to the almost total destruction of pancreatic $\beta - cells$ by $T - cells$.
The goal of diabetes treatment is to normalize the blood glucose levels with diet, exercise and medication. Generally the diabetologists give to all the patients, different and specific blood sugar targets based on their particular medical situation.

Hyperglycemia

Hyperglycemia is defined as a condition in which an excessive amount of glucose circulates in the blood plasma.
In people with diabetes, there are two different types:

1. *Fasting hyperglycemia*, which is a phenomenon that may be due to dysregulation of some hormonal patterns resulting in an increase, about 130 mg/dl, of hepatic glucose;

2. *Postprandial hyperglycemi*a, which arrives to high values of blood glucose (more than 180 mg/dl) and occurs after the meal;

Because of insulin deficiency, patients with T1DM often have elevated glucose concentrations in their blood.
As it has been said previously this important increase occurs because glucose fails to enter into the cells, and at the same time the liver continuously makes glucose by glycogenolysis and gluconeogenesis. The result of the insulin deficiency is that lipolysis and ketone formation aren't stopped, so the fatty acids increase and many of them are then converted by the liver into ketones, which are released into the blood. If the ketons in the blood are above 0.6 $mmol/L$, it occurs the so-called ketoacidosis and appropriate interventions must be taken.

Hypoglycemia

Hypoglycemia is defined as an abnormally low plasma glucose concentration. These very low values are due to some relative uncommon disorders such as a defect in one or more glucose regulatory control or an excess of insulin.
This condition can carry on a different amount of symptoms that can start from trembling, high heart rate, headache, state of confusion and more serious brain effects, including convulsions and coma.

1.2 The Artificial Pancreas

The technological improvements and the ongoing studies on insulin therapy and glucose monitoring have not yet led to a final therapy solution to the challenge related to the loss of insulin secretion [3]. The result is the ever present risk of long-term hyperglycaemia and not so uncommon hypoglycaemic events. A surgical possibility for the re-establishing, close to physiological, of the blood glucose control is the restoration of insulin secretion by pancreas or the islet transplantation: both of these solutions are not without risks and of the outcome still uncertain.
An alternative solution was proposed about 30 years ago and took the name of **Artificial Pancreas** ($\boldsymbol{AP}$). This system for closed-loop control of blood glucose in diabetic patients combines a glucose sensor, a pump of insulin and a control algorithm which decides how to adjust both the intravenous infusions of glucose and of insulin.
During the past decade a lot of enhancement were made, improvements involving

the technology, with the growing miniaturization of the system components and the robustness of the communication signals (Wireless - Bluetooth) among the different devices and involving the algorithm in which it's based the entire system. However, medical supervision remains necessary.
One of the final purposes of the project is to help the patients and the medical - engineering group that work on the Artificial Pancreas, warning with appropriate alarms in case that some failures happen during the utilization, as it will be better specified in the following; this thesis continue what Facchinetti et al. [1] started last year, analyzing these problems with simulated data.
As mentioned above the Artificial Pancreas is composed by 3 essential elements which are briefly described below.

1.2.1 The DiAs

In the early closed-loop control systems, the laptops were essential to run the control algorithms. In addition the laptops were wired to the sensor receiver and insulin pump [4]. Therefore, the utilization of this system was limited necessarily to the hospital. During the last years, the increase in computing power of smaller devices made possible, first the idea, then the realization, of a wearable AP. This step was of great relevance for the entire project and right now the control algorithms are implemented in JAVA (.apk package) by the Pavia and Virginia engineers, and installed on a Galaxy Nexus Device. Here the Diabetes Assistant (DiAs) was born. The Android operating system, running on these devices, was modified to satisfy the demands of medical use and was approved by the FDA. Thus, the graphical user interface was designed to be clear and intuitive for the patient which will be educated soon to use it at home, in the final phase of the clinical trials called, *AP@Home*.
Note that the DiAs system has been used in 3 clinical trials finalized to test the proper functioning of the state-of-art AP, to which i take part during the period of the thesis. In Figure 1.2 a screen of the DiAs User Interface is shown.

More details on DiAs initialization, functioning and seafty protocols are reported in Appendix A.

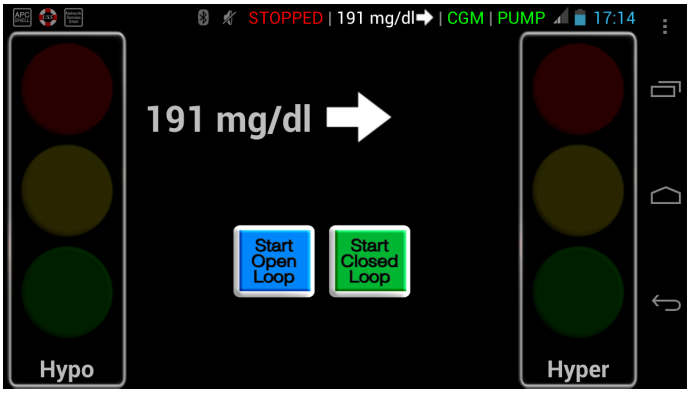

Figure 1.2: DiAs Stopped Mode.

1.2.2 The Continuous Glucose Monitoring - CGM

The **C**ontinuous **G**lucose **M**onitoring, **CGM**, system is an electronic device that measure physiological glucose levels. In Figure 1.3 it can be seen the Dexcom®G4, the device that was used in all the clinical trials cited before. As all others CGMs produced until now, it's made of a glucose sensor *needle-type* and based on the glucose-oxidase technology, with which it measures glucose levels of the interstitial fluid. It has a bluetooth transmitter which communicates the glucose readings both with the Dexcom reciver and mostly with the DiAs.

Figure 1.3: CGM sensor and reciver, Dexcom G4.

Only in the last years the CGM systems allowed their reliable use in the project AP. For the success of the latter, there are in effect a lot of important factors that must be considered about the utilization of these devices.

As it can easily be imagined, is of fundamental relevance to obtain a precise estimate of blood glucose level by the sensor, being one of the most important inputs of the control algorithm. But this estimation is done with the glucose in the interstitial fluid while the metabolic control is based on plasma glucose concentration. Thus, this physiological difference must be considered when applying an AP. The most recent of them, such as Dexcom G4, achieve about 10% mean absolute relative difference between the two types of glucose, over the entire physiological range [4]. With the currently available CGM systems, glucose sensing can be considered reliable on 5-7 day periods.

1.2.3 The continuous subcutaneous insulin infusion - CSII

The other key element to which the DiAs must be connected is what is commonly called insulin pump.
This device is, more specifically, a **C**ontinuous **S**ubcutaneous **I**nsulin **I**nfusion system, **CSII**, which injects a sort of short acting insulin, delivered via a subcutaneous needle and is connected to a reservoir of insulin by a catheter and a command module.
During the clinical trials, the DiAs was paired with two different pumps, see Figure 1.4, the t:slim by Tandem [t:slim]. the ACCU-CHEK Combo by ROCHE [ACCU-CHEK Combo].

(a) ACCU-CHEK Combo

(b) Tandem

Figure 1.4: Continuous Subcutaneous Insulin Infusion.

1.3 Aim of the thesis

The Artificial Pancreas is a complex system composed by different devices, which can be occasionally affected by malfunctioning. For instance, the application of a pressure on the CGM sensor produces on the CGM output a significant underestimation of the glucose concentration, as well as the occlusion of the catheter of the CSII pump produces an increase of the glucose concentration. Also human errors are possible. For example, the diabetic patient using the AP system can accidentally insert wrong information about the quantity of the meal that he/she is going to eat. All these failures are critical for the calculation of the optimal insulin infusion by the AP controller and, in some cases, dangerous for the safety of the patient.
The aim of this thesis is the development of a failure detection method able to detect and classify such failures and generate failure alerts in real-time, and to test it in an in-silico environment able to reproduce most of the critical failures that could happen during in-vivo experiments.

Chapter 2 presents the description of the CGM and CSII failures and some of the most critical human errors that can happen during the utilization of the Artificial Pancreas.

Chapter 3 reports a briefly overview of the Kalman Filter, the "instrument" used to implement the Failure Detection Method, and the way in which it is used for the purpose of this thesis.

Chapter 4 illustrates the Fault Detection Method, presenting the model employed for the detection, the need to use personalized models to achieve better performance and the way in which the model is transformed into a Kalman predictor to generate on-line retrospective predictions coupled with different alarm strategies.

In *Chapter 5*, the data-set used for the simulations and the method of analysis are presented.

Finally in *Chapter 6* it is shows the results obtained for each kind of simulated fault with the corresponding statistical analysis.

Chapter 2

An introduction to failures in AP system

The Artificial Pancreas is a system composed by different devices (smartphone, CGMs and CSIIs) and that expected an iterative utilization by the user (insertion of information about the meals and on cases of hypo/hyper-treatment).
Despite the therapeutic advantages of using CSII and CGMs, their use has been associated with different risks too. These could be due to some technical malfunctioning of the devices, or to some movements of the patient which accidentally cause an obstruction of the pump/sensor components or even to a pressure of the zone in which the devices are operating.
All these situations can result in a more or less strange and dangerous behaviors of the glycemic control.
Moreover, also the interventions of the users can lead to some errors that are then fatal for the proper DiAs functioning.
In this chapter, some failures of the CGM system and of the CSII system are presented. Futhermore, it is introduced also one of the most common human error, that is the wrong meal announcement.
The main difficulty of the identification of these faults, is that these may occur for different reasons but appear for several time in the same mode on the CGM output track, or they can verify themselves also some hours before that it can be possible to see their effect on the CGM signal.
It's possible to distinguish three important class of failures, (every detail on the realization of the faults, will be described in the Chapter 5), grouping several cases:

2.1 CGM sensor failures

The first class concerns the faults that occur on the CGM sensor. They are mainly related to biomechanic issues of the sensor-tissue interface [5], which create a loss of sensitivity within the sensor. The effect of such a loss is visible on the CGM time series as an understimation of the current blood glucose concentration.
These events are common especially at nighttime, when the patient while sleeping could apply a pressure on the sensor by rolling on it but also during the normal daily activities. When this happens, the glucose diffusion in the region of sensor application is altered causing a modification of the sensor sensitivity; moreover the corresponding compression artifacts distort the signal acquired.
This fault can last for a very short time so that is lost only one sample and in this case it is called *spike*. On the other hand it can last for quite some time so that is lost more than one sample and the fault is called *loss*. Both belong to the class of the compression artifacts and in Figure 2.1 and 2.2 can be seen two realizations of example:

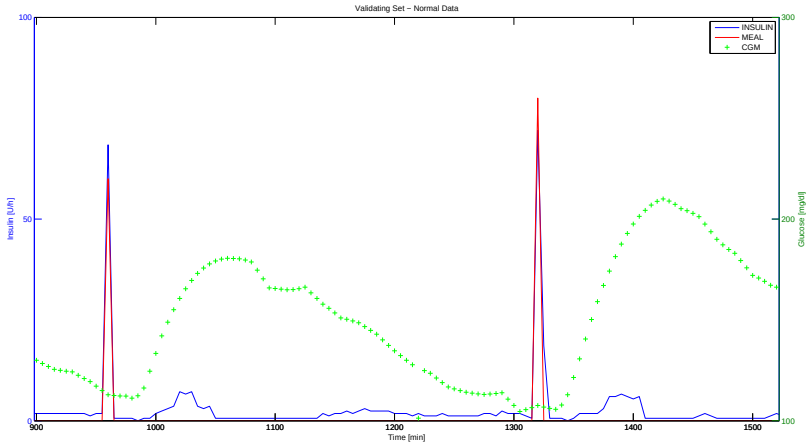

(a) A CGM spike results at $t = 1220$.

Figure 2.1: It can be seen as the value of the spike is quite lower than the CGM values nearby.

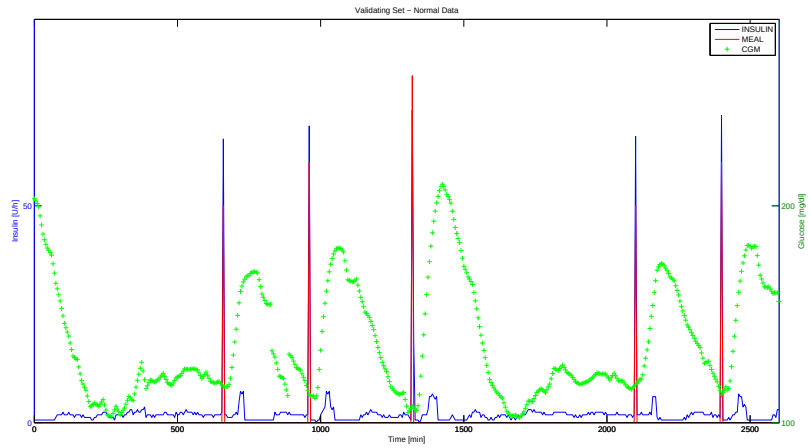

(a) A CGM loss of sensitivity starts at $t = 775$.

Figure 2.2: In the plot a loss of sensitivity results in 12 samples that are clearly underestimated by the sensor.

2.2 Meal and Meal-Bolus failures

The second class is about the errors of communications that could happen between the DiAs and the other devices. In the specific, it was considered the:

- wrong communication of the meal to the DiAs by the users (human error);
- insulin meal bolus delivered by the pump but not communicated to the DiAs (technological error);

Considering the first case. Up to this moment, patients use subcutaneous pumps for deliver to themselves the insulin bolus before a meal. To calculate the bolus amount they have to estimate the carbohydrates of their meal, CHO, and divide it for the carbohydrates-to-insulin ratio, $CR = \frac{CHO}{I}$, which is a fundamental patient-specific value, that can vary from meal to meal and that is provided by the diabetologist. Currently, the DiAs requires these two informations; the carbohydrates-to-insulin ratios are saved into the "*Insulin Profiles*" section that must be compiled by the bio-engineer or the doctor before to start any session, so this parameter can be considered not affected by any error. Instead errors could happen in the *meal announcement* procedure, see Chapter 1 for details, during which the patient ha to insert manually the CHO amount in the DiAs. Although this procedure is performed

typically under the supervision of the work team, some problems or unexpected errors could occur. For example an entry error due to different technical reasons, such as a little confidence with the touch screen; a miscalculation or just a too much hurry while inserting the data; the meal announcement is done correctly, but for some other external reasons, the patient can't eat his meal anymore (as in the case in which falls the dish to the waiter or the patient feels unwell). In all these unfortunate, but possible, events the Artifical Pancreas will operate with wrong data streams and so the subsequent release of insulin decided, would be either too high or too low.

The Meal - Bolus Failure is a fault involving the insulin pump.
In some cases, again for different reasons, it could happen that after the meal announcement the system does not detect the arrival of the entire or partial insulin bolus. In this scenario the patient received the right quantity of insulin, the one calculated after the meal announcement and correctly delivered, but the DiAs doesn't know this and so it probably wrongly increases the basal, believing that not enough insulin was given to the patient. This consequence is very dangerous beacause could leads to a very low level of blood sugar and so to a relative quickly hypoglicemia for the patient.

In Figure 2.3 can be seen two faulty events, the first one, (a), about the meal and the second one, (b), about the meal-bolus:

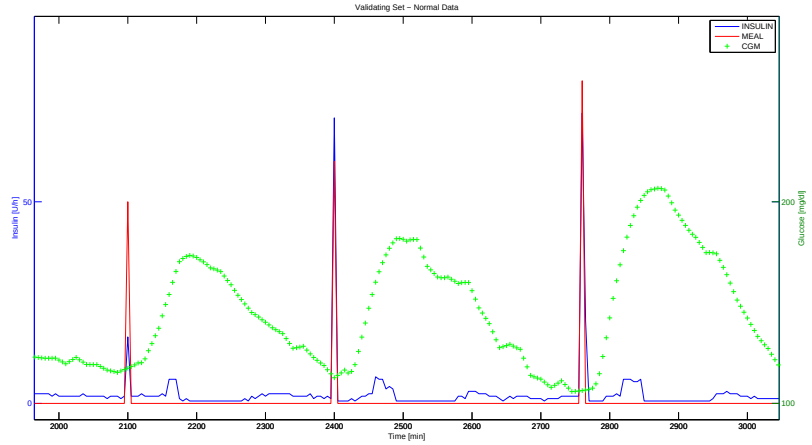

(a) A insulin bolus due to the meal at $t = 2100$ min which undergoes a decrease of 75%

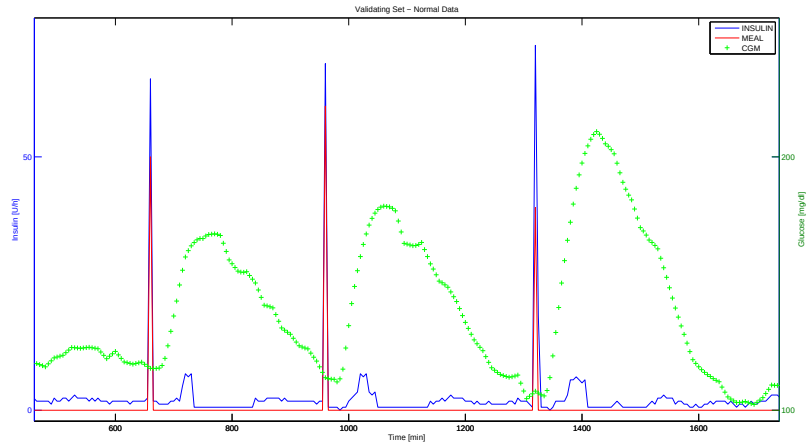

(b) A meal at $t = 1320$ min which undergoes a decrease of 50%

Figure 2.3: In the (a) and (b) plots the blue lines represent the insulin while the red lines the meals. The two decreases are evident in both the cases.

2.3 CSII pump failures

The last class of fault relates to the pump failures. This is the most challenging considered scenario, beacuse of the delay that occurs between the event and the effect that it produces on the glucose concentration (due to delays in insulin absorption and action). Here it is considered the case of absence of basal insulin delivery by the

pump. In AP system, the insulin pump is controlled wireless by the Galaxy Nexus device in which runs the control algorithm. A situation that could happen during various activities of the patients throughout the day or also the night, is that the connectivity between these two devices is lost and consecutively the insulin delivery should be interrupted or reduced. This is a very challenging scenario, because the effects of this reduction can be observed on the glucose concentration only tens of minutes later the fault, the time it takes to wait the delay due to insulin absorption and to the insulin action.

The basal failure can be critical both for the correct functioning of entire system, which if it doesn't know how much is the real amount of insulin delivery it wouldn't make the right estimate, and for the safety of the patient that can be a risk of hyperglycemia and of ketoacidosis due to the lack of basal insulin for a long time.

Another unlucky possibility, is the one that can be seen in Figure 5.8. The basal insulin is higher than what is expected and this situation can verify if there are some technological issues, especially during the testing of new insulin pump that can require different settings from others to work in the right way, or if the patient informations that were inserted to the DiAs at the starting of the session were wrong.

In the following Figure 2.4 is shown how it's difficult to see, without any help, the decrease of the basal insulin that results for 5 hours, starting from $t = 1520$ min.

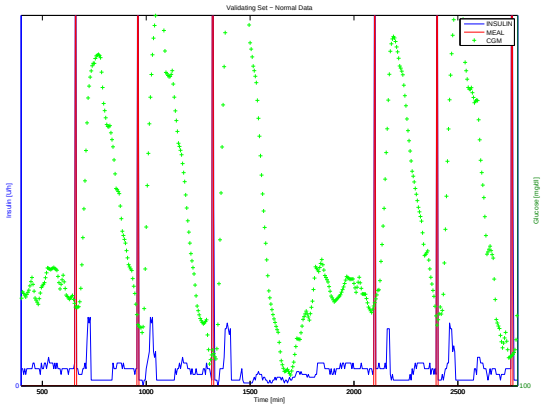

Figure 2.4: The basal fault starts at $t = 1520$ and its duration is 5 hours. It was decreased the basal value by 50%.

Chapter 3

The Kalman Filter

The Kalman Filter is an optimal recursive data processing algorithm.
It is fundamentally a set of mathematical equations that are used to implement the so called Kalman Predictor, an algorithm that processes all available measurements at time t to perdict the *t+1* value of the system output, taking into account the noises, the statistical description of the model and the knowledge of the system and of his dynamic.
It is optimal in the sense that among the linear estimators, it minimizes the variance of the prediction error.

3.1 The Discrete Kalman Filter

Before to start any considerations on the filter and its implementation, it is important to discuss some property of the glucose-insulin system allows to effectively applicability the Kalman Filter algorithm:

1. The glucose-insulin system, is not-linear. However, it is possible to obtain an approximate linear description of it, sufficiently accurate for the purposes, as will be demonstrated in the theis.

2. Such a model can accounts for some aleatory, with the inclusion of two terms, v_t for the model and w_t for the measurement, corresponding to two white noises.

3. The considered white noises, v_t and w_t, have a probability density fairly symmetrical and are unimodals.

The Kalman Filter requires a state-space model for describing the signal dynamic, that combine deterministic-stochastic system. Considering now:

$$\begin{cases} x_{t+1} = Ax_t + Bu_t + v_t & \text{with } \mathrm{Cov}(v_t) = Q \\ y_t = Cx_t + Du_t + w_t & \text{with } \mathrm{Cov}(w_t) = R \end{cases} \tag{3.1}$$

where x_{t+1} is the state vector at time $t+1$, y_t is the estimate at time t, u_t is the input vector, $v_t \sim N(0, Q)$ is the model noise which represents the disturbances entering the system, where Q is its covariance matrix and $w_t \sim N(0, R)$ is the measurement noise which represents the uncertainty in the system observations, where R is its covariance matrix. It's noteworthy that the model is completely specified by the matrices A,B,C,D,Q,R, the input and output vectors are measured while the noises are unmeasurable but are assumed white and zero mean.
Futhermore, $Q \succ 0$ and $R \succ 0$. The two covariance martices realted to the noises are definite positive, so it is guaranteed the invertibility of the matrix and the correctness of the algorithm.

In many concrete problems the model and measurement noises are often uncorrelated but it may happen that they are, even minimally [6]. In this case their covariance matrix is the following:

$$E\left\{ \begin{bmatrix} v_t \\ w_t \end{bmatrix} \begin{bmatrix} v_s^T & w_s^T \end{bmatrix} \right\} = \begin{bmatrix} Q & S \\ S^T & R \end{bmatrix} \delta(t-s)$$

Now the noise can be rewritten introducing:

$$\tilde{v}_t = v_t - \hat{E}[v_t|w_t] = v_t - SR^{-1}w_t$$

where $\hat{E}[.|.]$ is a minimum variance linear estimator.
Thus the variance of this noise $\tilde{v}_t$ is:

$$\bar{Q} = Q - SR^{-1}S^T$$

and reconsidering the system model it can be written:

$$w_t = y_t - Cx_t - Du_t$$

Replacing v_t:

$$\begin{cases} x_{t+1} = Fx_t + SR^{-1}y_t + \bar{B}u_t + \tilde{v}_t \\ y_t = Cx_t + Du_t + w_t \end{cases} \tag{3.2}$$

with:

$$F = A - SR^{-1}C \quad \bar{B} = B - SR^{-1}D$$

It should be noted first that now the noises, w_t and $\tilde{v}_t$ are no longer correlated thanks to a new term that appears in the state equation: $SR^{-1}y_t$. This is a feedback from the output to the state and is called *output injection*. Second, if the S matrix is null it is obtained the previous system where the noises are already uncorrelated.

3.2 The 2 Steps Algorithm

The iterative algorithm which leads to the evaluation of the output consists of 2 steps:

1. Two equations of *Predictions* that *predict* the future state $\hat{x}_{t+1|t}$ and the error covariance matrix $P_{t+1|t}$;
2. Two equations of *Measurement Update* that *correct* the estimates just done, obtaining $\hat{x}_{t|t}$ and $P_{t|t}$;

The *Prediction* equations are used to compute at time t of the future state $\hat{x}_{t+1|t}$ and error covariance estimates at time $t+1$, $P_{t+1|t}$. These estimates are corrected with the upcoming measurement, by the second step of the algorithm, allowing to obtain an improved a posterioroi estimate. That's why the resulting algorithm can be classificated as a predictor-corrector algorithm.

After each cycle the process is repeated with the previous a posteriori estimates used this time to predict the new a priori estimates.

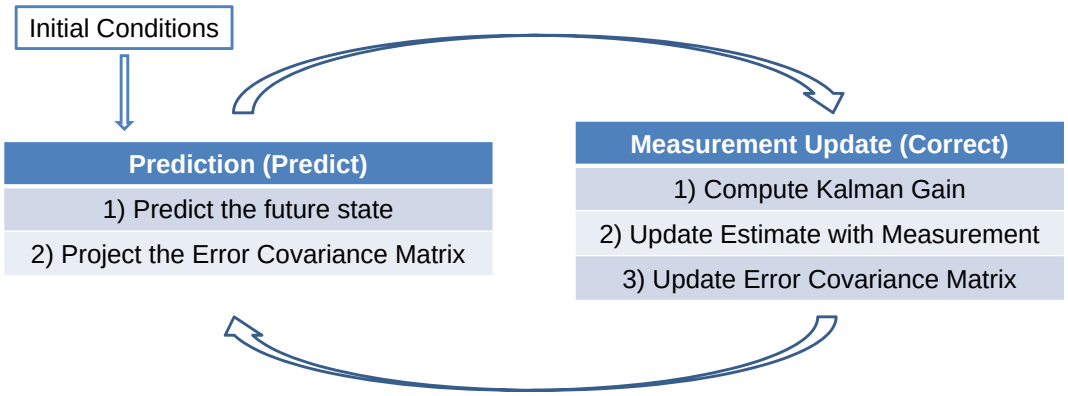

Figure 3.1: High Level Diagram of Kalman Filter Algorithm.

To better understand the elements of the algorithm [7], here are introduced the two components:

- $\hat{x}_{t+1|t}$ which is the state estimate at step t calculated with the knowledge of the output measurements up to time t.

- $\hat{x}_{t|t}$ which is a posteriori state estimate always calculated at step t but with also the knowledge of the measureament at time $t+1$.

So it can be searched an equation that calculates the a posteriori estimate $\hat{x}_{t|t}$ such as a linear combination of the a priori estimate $\hat{x}_{t+1|t}$ and of the weighted difference between the actual measurament y_k and the prediction of the measurament, given by $C\hat{x}_{t+1|t} + Du_t$. It follows that $\hat{x}_{t|t} = K(y_k - C\hat{x}_{t+1|t} - Du_t)$.
$y_k - C\hat{x}_{t+1|t} - Du_t$ is called "*innovation*" and reflects the difference between the state predicted and the measurament z_k.
The K variable is called "*Kalman Gain*" and is calculated so as to minimize the a posteriori estimate error covariance P_k, given by $P_k = E[\epsilon_k \epsilon_k^T]$ where $\epsilon_k \equiv x_t - \hat{x}_{t|t}$. A possible form, coming from the theory of the Kalman equations, is $K = P_{t|t-1}C^T(CP_{t|t-1}C^T + R)^{-1}$.

It follows the pseudocode of the algorithm:

$K_0 \leftarrow P_0 C^T (C P_0 C^T + R_0)^{-1}$;
$\epsilon_0 \leftarrow y_t - C x_0 - D u_t$;
$\hat{x}_{t|t} \leftarrow x_0 + K_0 \epsilon_0$;
$P_{t|t} \leftarrow P_0 - K_0 C P_0$;
$\hat{y}_1 = C \hat{x}_{t|t} + D u_1$;
for $t = 1$ **to** $T_{fin} - 1$ **do**
  $\bar{Q} = Q - S R_t^{-1} S^T$;
  $F = A - S R_t^{-1} C$;
  $\bar{B} = [B - S R_t^{-1} D, \quad S R_t^{-1}]$;
  $\hat{x}_{t+1|t} \leftarrow F \hat{x}_{t|t} + \bar{B} [u_t \quad y_t]^T \Rightarrow$ *Time Update*;
  $P_{t+1|t} \leftarrow F P_{t|t} F^T + \bar{Q} \Rightarrow$ *Time Update*;
  $K = P_{t+1|t} C^T (C P_{t+1|t} C^T + R_{t+1})^{-1}$;
  $\epsilon = y_{t+1} - C \hat{x}_{t+1|t} - D u_{t+1}$;
  $\hat{x}_{t|t} = \hat{x}_{t+1|t} + K \epsilon \Rightarrow$ *Measurement Update*;
  $P_{t|t} = P_{t+1|t} - K C P_{t+1|t} \Rightarrow$ *Measurement Update*;
  $\hat{y}_{t+1} = C \hat{x}_{t|t} + D u_{t+1}$;
end

Here are highlighted two aspects that will be fundamental for the implementation of the Fault Detection Method that will be discussed of *Chapter 4*:

1. Large values of R_t means that will be not used y_t in the estimation and that: $F \approx A$, $\bar{Q} \approx Q$, and $\bar{B} \approx B$;
2. Large values of R_{t+1} means that $K \approx 0$ and therefore $\hat{x}_{t|t} = \hat{x}_{t+1|t}$ and $P_{t|t} = P_{t+1|t}$.

3.3 An example of explanation

To clearly explain and better understand the theory of Kalman Filter, it's now reported an easy example focused on the glucose-insulin system.
Supposed that are available the glucose measuraments and the insulin input just as reported in the following Figure 3.2:

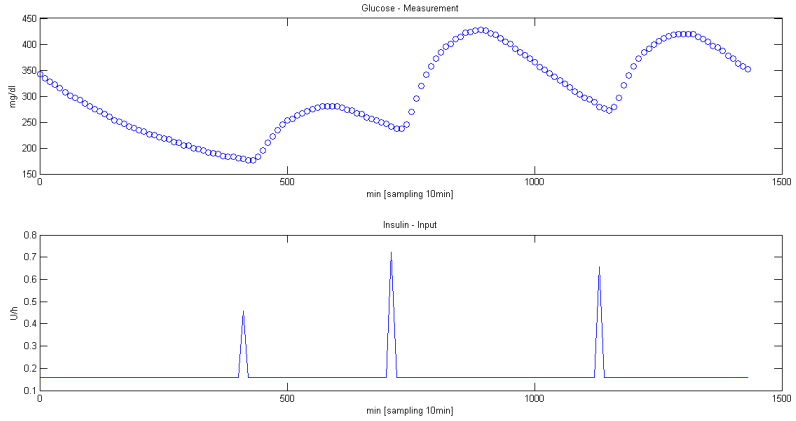

Figure 3.2: Measurements and input.

After the identification of the matrices of the space-state system reported in 3.1 (this step will be discussed in detail in chapter 4), the calculation of the equations can be strated. Figure 3.3 shows six cycles of the algorithm.
First of all, it's initialized the state x_0 to 0 and P_0 as a large error covariance matrix since the accuracy of the state estimate is very low. In fact the first subfigure *First Step* shows that when it starts, the algorithm considers true the measurement but his error covariance matrix has high value.
After this process, the algorithm predicts the future state, weighing the actual state with the A matrix and update the error covariance matrix considering the old one and the Q model covariance matrix.
Then it follws the calculation of the kalman gain, of the innovation and the adjustment of prediction with the measurement information.
Thus, it can be calculated the final output, using this final result for the state. The second subfigure *Second Step* shows how the prediction was higher then the final filtering, that lowers the value because the mesaurement result lower then the prediction.
As can be seen in the other subfigures, the measurement update is equal to the prediction when the filter is operating and when there aren't faults that occurred. This is an aspect that will be discussed in *Chapter*4 when it will be discussed the process used for the identification of the model and its validation.
In the final subfigure *Final Result* it can be seen in black the real measurements and in green the entire prediction of the output using the Kalman Filter.

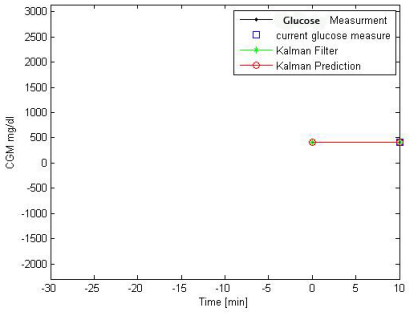

(a) First Step

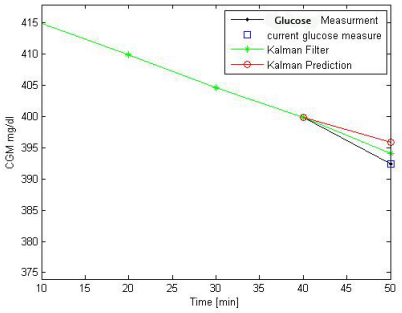

(b) Second Step

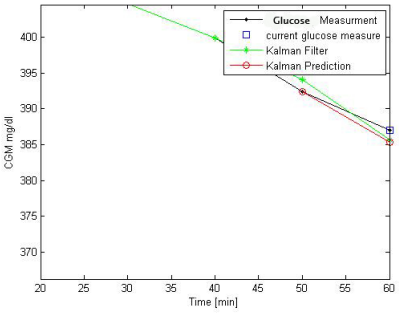

(c) Third Step

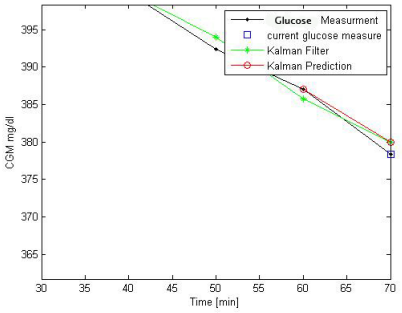

(d) Fourth Step

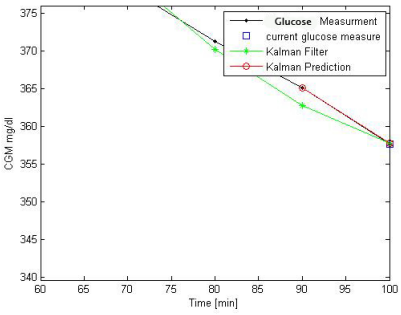

(e) Fifth Step

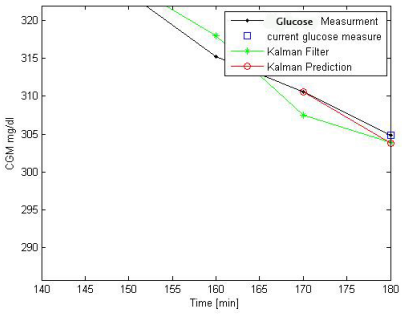

(f) Sixth Step

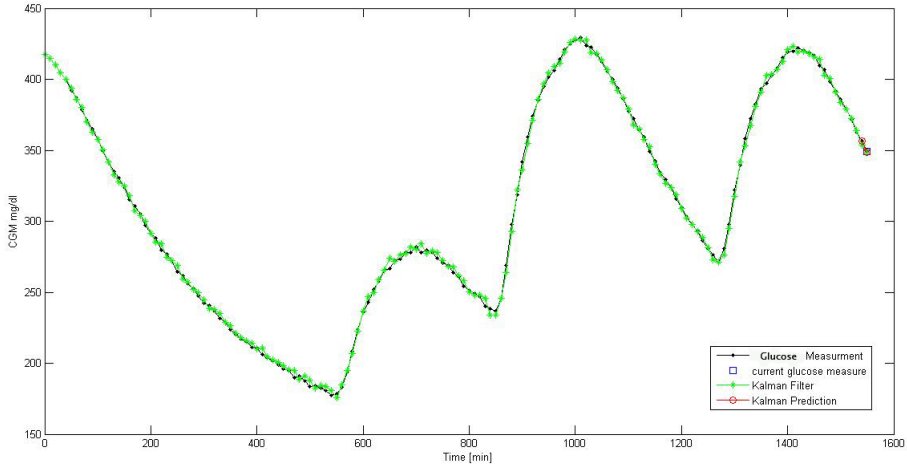

(g) Final Result

Figure 3.3: Prediction and Measurement Update.

Chapter 4

Fault Detection with Kalman Filter

In Figure 4.1 it's shown the block-scheme that describes the fundamental steps of the Fault Detection Method.

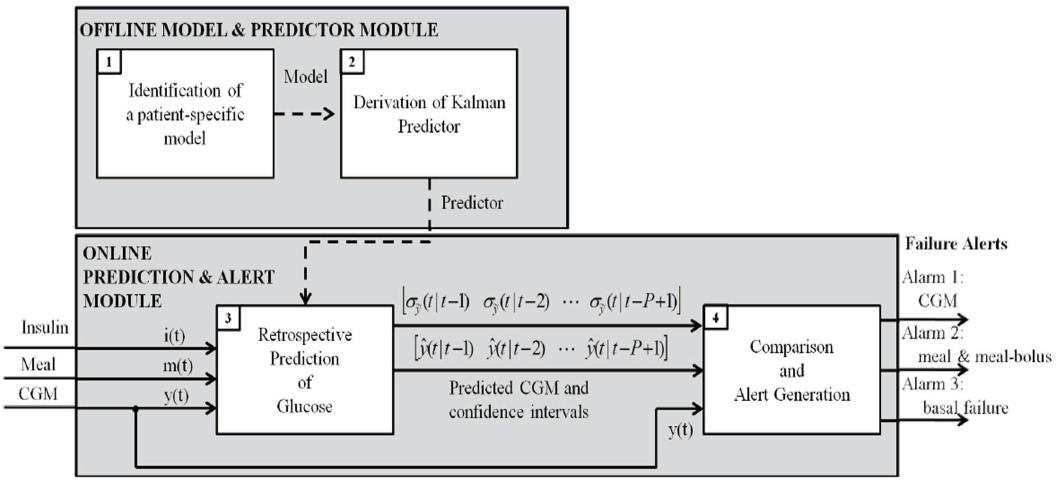

Figure 4.1: Block Scheme of the FDM

First of all, two distinct modules can be identified.
The first one, called **MODEL & PREDICTOR** and located at the top of Figure

4.1, consists of two blocks executed off-line. The *block 1* identifies a patient-specific linear model which describes the relationship between the system output, glucose concentration measured by CGM, and the inputs, insulin injected by the CSII and amount of carbohydrates ingested. The datails on the identification process are reported in paragraph 4.1. In *block 2*, using the identified model, it's derived the Kalman Filter Predictor. The latter is then used in the second module of the block-scheme, called **ONLINE PREDICTION & ALERT**. This module responsible of the alerts generation, consists of two blocks and works on-line. In block 3, the predictor is fed with the CGM measurements, the insulin delivered by CSII and the meal data and it provides at any time t a retrospective prediction of the glucose concentration, explained in paragraph 4.2. Finally in block 4, are produced the alarms in 3 different ways which will be explored in paragraph 4.3.
The main purpose of this study is that to generate consistent on-line alarms when the simulated failures are detected by the algorithm developed.

4.1 Personalized Models

One of the main problem of this study, concerns the identification of the model.
It is a very challenging step because of the great variability of the 100 subjects, which forces to make an identification for each one.
Given the two inputs, corresponding to the injected insulin and to the meal, and the output measurements, that is the CGM signal, it must be obtain the matrices for the state-space model:

$$\begin{cases} x_{t+1} = Ax_t + Bu_t + v_t & \text{with } \mathrm{Cov}(v_t) = Q \\ y_t = Cx_t + Du_t + w_t & \text{with } \mathrm{Cov}(w_t) = R \end{cases} \tag{4.1}$$

that describe the system.
To operate the identification, it was used *N4SID*, **N**umerical algorithms for **S**ubspace **S**tate **S**pace **S**ystem **I**dentication, a method which estimates the state-space model using a subspace method [8].
For the development of the code it was used Matlab®(Version R2012b, The Math Works, Inc, Natick, MA) and in particular for the identification of the unknown matrices, it was used its function *n4sid*.
The identification was made on clean data that is on data without any transient

failures and for each subject, it was performed one identification. To do this, 3 days of data were used. Once obtained the matrices, it was carried out the validation to complete the identification process, using the remaining 2.5 days.
The identification process is complicated by the close correlation between the two inputs. In fact every time a meal occurs, at the same time a bolus of insulin appears. For the identification algorithm, becomes really difficult to understand the difference between these two signals, that are both largely positive in correspondence of a rising of the glycemia.
To confirm this, the impulse responses of the two inputs, after the *N4SID* identification performed on these *unprocessed data*, were very oscillatory and a number of times with the wrong signs. In fact, it is to be expected that the insulin impulse response will be negative and the meal impulse response will be positive. Instead, as can be seen in Figure 4.1 (a), the insulin input has the wrong sign.

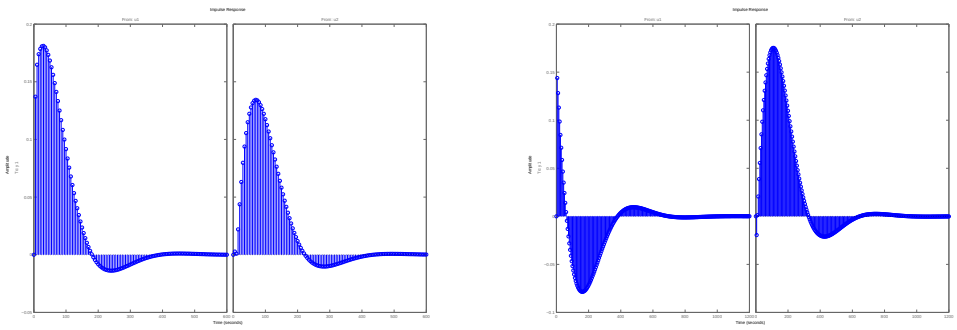

(a) Impulsive Response identified on normal data

(b) Impulsive Response identified on trasnformed data

Figure 4.2: Impulsive responses of the identificated system: the (a) plot shows that the first input (insulin) has a wrong sign when normal data are used for the identification of the model. The impulsive response in (b), proves that their trasformation is necessary.

This is a considerable problem and to try to solve it, it was proposed an input transformations on the data which will be described briefly here. At each time t, it were calculated the so called *feedfoward insulin*, i_{ff}, which was equal to the basal insulin at time t, plus the meal divided bt the CR: $i_{ff} = i_b + m/CR$. So now, subtracting to the insulin the *feedfoward insulin*, it is get a new signal, called $\Delta Insulin$, $\Delta i = i - i_{ff}$ which still has small peaks at the same times of the meals, but its

evolution is very different from before, it can also have negative values and this help the identification process. Also to the glucose signal was subtracted a *basal glucose* parameter that was imposed equal to $120mg/dl$ as the normal glicemical target, $\Delta CGM = CGM - CGM_{basal}$.
These transformations helped to identify the model, step clearly critical to the development and analysis of Fault Detection Method.
Figure 4.1 (b) shows that the impulsive responses, after the trasformations applied to the data, are definitively better than the one which is obtained from the normal data even if there are still some oscillations. It is to note that if the matrices obtained with the untrasformed data had been used, the model would not have distinguished a meal from an insulin injection.

4.2 The On-line Predictions

In *block 3* the Kalman Predictor reviewd in the previous chapter and computed in *block 2*, is used in real time for the calculation of a *retrospective prediction*, [1], it was computed $\forall \quad t \qquad and \qquad \forall \quad k \in [1, ..., P]$

$$\hat{y}_{pred}(t-P+k|t-P) = CA^{k-1}\hat{x}_{t-P+1|t-P} + C\sum_{i=1}^{k-1} A^{i-1}Bu_{t-P+i} + Du_{t-P+k} \quad (4.2)$$

where the input data (CSII and the meal) are used up to time t while the CGM data acquired where used till time $t-P$, where P is the Prediction Horizon measured in steps.
It is called retrospective prediction because all measurements collected from time t-P+1 to t are not used.
More in detail, the **P**rediction **H**orizon $PH = P \cdot T_{samp}$ is the term used to indicate how much steps forward the prediction looks at.

For each predicted values, it is calculated in *Block 3* an estimate of the convidence interval as:

$$[\hat{y}_{pred}(t-P+k|t-P) - m \cdot \sigma_{\hat{y}_k} \quad , \quad \hat{y}_{pred}(t-P+k|t-P) + m \cdot \sigma_{\hat{y}_k}] \qquad k = 1, ..., P \quad (4.3)$$

with:

$$\sigma_{\hat{y}_k} = \sqrt{CP_{t-P+k|t-P}C^T + R}$$

$\sigma_{\hat{y}_k}$ is the standard deviation (SD) of the k-step ahead prediction value while m is an important parameter that will be determinated equal to 3 with the ROC analysis, in the first paragraph of Chapter 6. Moreover, the terms $P_{t-P+k|t-P}$ is the covariance matrix of the estimated state vector $\hat{x}(t-P+k|t-P)$.
Different **P**rediction **H**orizons were considered during the detection of the different fault.
In the first plot of Figure 4.2 is shown the 1-step prediction, $P = 1$ that is $PH =$

5 min, used in the first two alarm startegies, that will be explained in the next paragraphs.
In the other plots can be seen instead, the result on a single subject, using a $PH = 4$ hours, the same one used in the third alarm strategy which will be defined in 4.3.3.
In plot (b), the first step of the algorithm is represented: since no a priori information is available, $P_0 = \infty$ and hence the starting point is exactly on the measure, with a very wide confidence interval. Moreover, it can be seen that the prediction, even if very long, is able to predict very well the ups and downs of the glycemia, see plot (c), (e) and (g). What happen when the algorithm has to predict the slop variations is very interesting. As it is shown in plot (d) and (f) the prediction follow effectively the signal.
Finally in plot (h), is shown the great prediction during the nighttime.

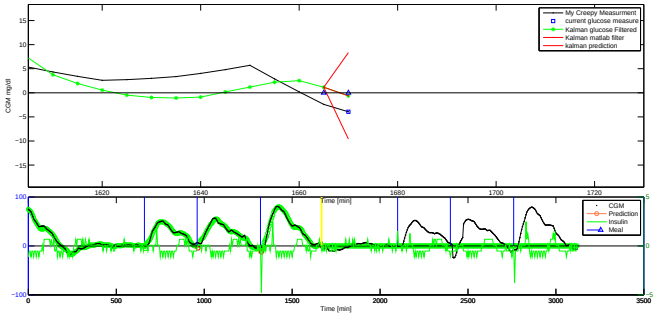

(a) Prediction 1 step forward

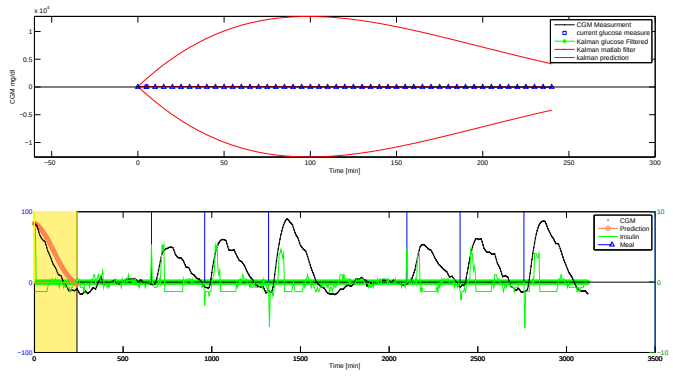

(b) Prediction 48 steps forward - initialization

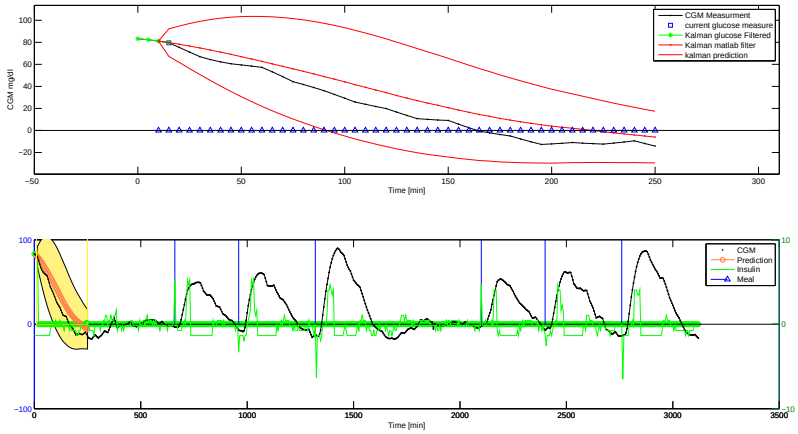

(c) Prediction 48 steps forward - after the initialization

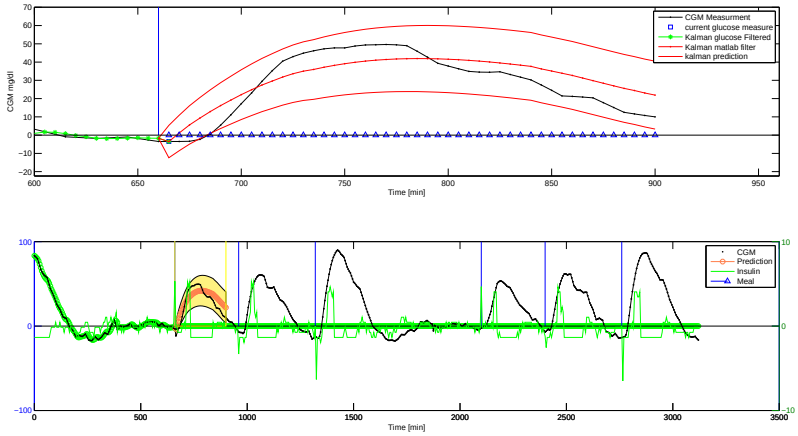

(d) Prediction 48 steps forward - the first meal

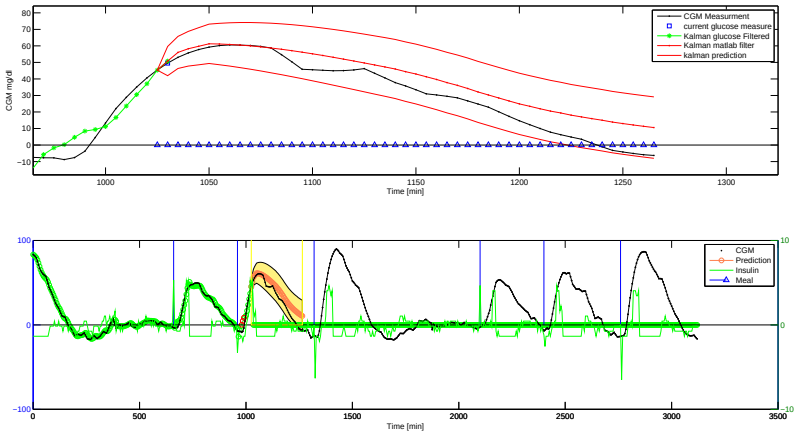

(e) Prediction 48 steps forward - descent

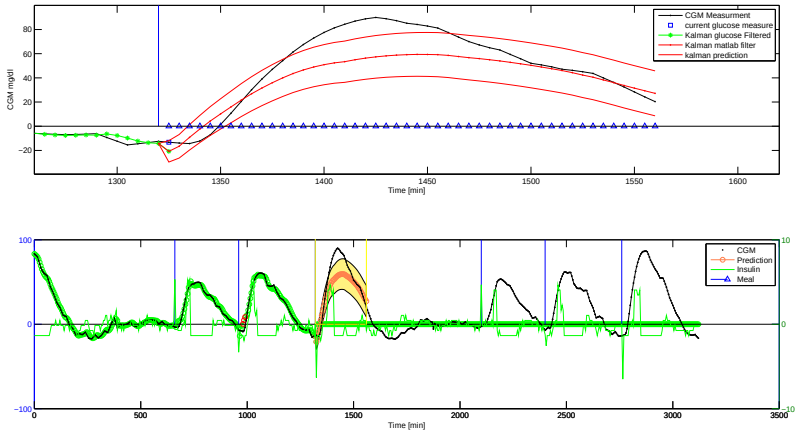

(f) Prediction 48 steps forward - another meal

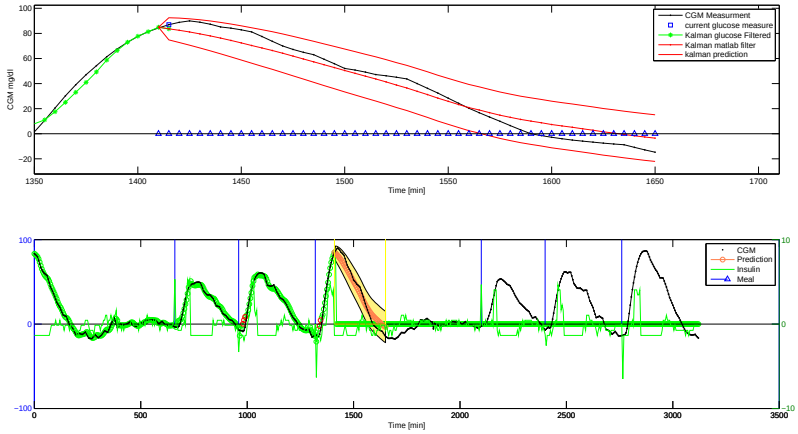

(g) Prediction 48 steps forward - the faster descent

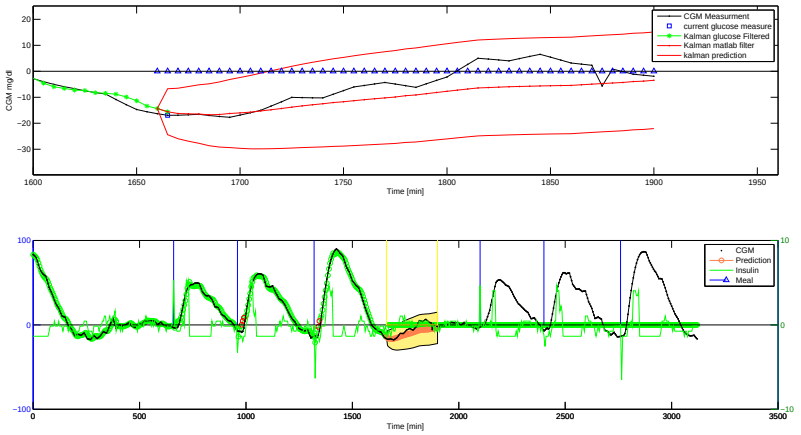

(h) Prediction 48 steps forward - nigth

4.3 The Alarm Startegy

Apparently, the various faults described previously can not be detected in the same way. There are too many differences in the amplitude, the duration, and especially, the time with which they act on the system. A spike, for example, is both less serious and more easily detectable than a basal fault.
For this reason have been designed more alarm strategies who warn on different events:

- *Alarm CGM*: that warns on the compression artifacts (spikes and losses);
- *Alarm Meal and Meal-Bolus*: that warns on failures involving a wrong "meal announcement" or a wrong bolus of insulin in corresponding of a meal;
- *Alarm Basal Failure*: that warns if there are some problems on the delivering of the basal insulin;

4.3.1 Alarm 1 - CGM

The Fault Detection Algorithm in these cases, works as follow (in Figure 4.8 the scheme can help to follow these steps) :
At each time t the algorithm calculates the retrospective prediction $\hat{y}_{pred}(t+1|t)$ and make a direct comparison with the measurement that it received. If the measurement is into the bounds calculated in *block 3*, it is reasonable to think that everything is working fine.
However, if the prediction is out from the calculated bounds a faulty sample is detected.

If the sample is deemed faulty, the R_{t+1} matrix is set with large values so that the measurement isn't used because:

$$\hat{y}_{t+1} = C\hat{x}_{t|t} + Du_{t+1} \qquad \text{where} \qquad \hat{x}_{t|t} = \hat{x}_{t+1|t} + K\epsilon$$

$$\text{where} \quad K = P_{t+1|t}C^T(CP_{t+1|t}C^T + R_{t+1})^{-1}$$

$$\text{and} \quad \text{so} \qquad \hat{x}_{t|t} \approx \hat{x}_{t+1|t} \qquad \text{and} \qquad \hat{y}_{t+1} = C\hat{x}_{t+1|t} + Du_{t+1}$$

and the sample is possibly a spike.
If at the next time the prediction re-enters in the confidence interval, the past sample is classified as spike, see Figure 4.3.
If however, the next measurement is still out of bounds the counter increasing his value and the samples are calssified as a loss, which could also be partial such as in Figure 4.4.
Considering now the Figure 4.3 where the CGM signal has an evident spike at time $t = 1510min$.
In cyan there is the final result of the entire prediction using the algorithm described above. As can be seen in the first plot, which is the zoom of the faulty area, the prediction is quite different by the wrong measurement that arrives from the CGM. These two conflicting informations allow to recognize if something strange is happening, and in this particular case the spike has been identified.

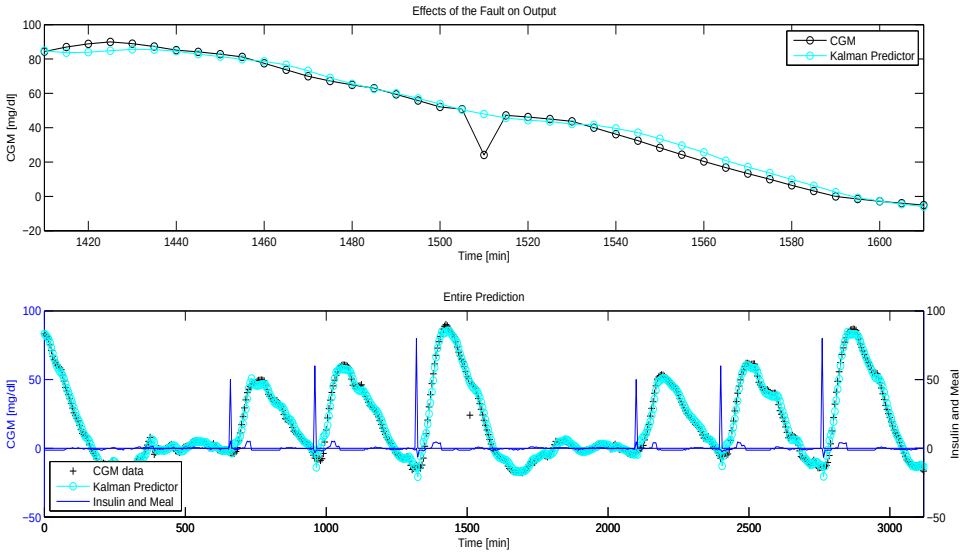

Figure 4.3: Prediction of Spike Failure.

Similar considerations can be done for the losses. Figure 4.4 shows how the algorithm doesn't agree with the measurements that arrive from the simulated glucose sensor, and it predicts a different dynamic of the CGM signal.

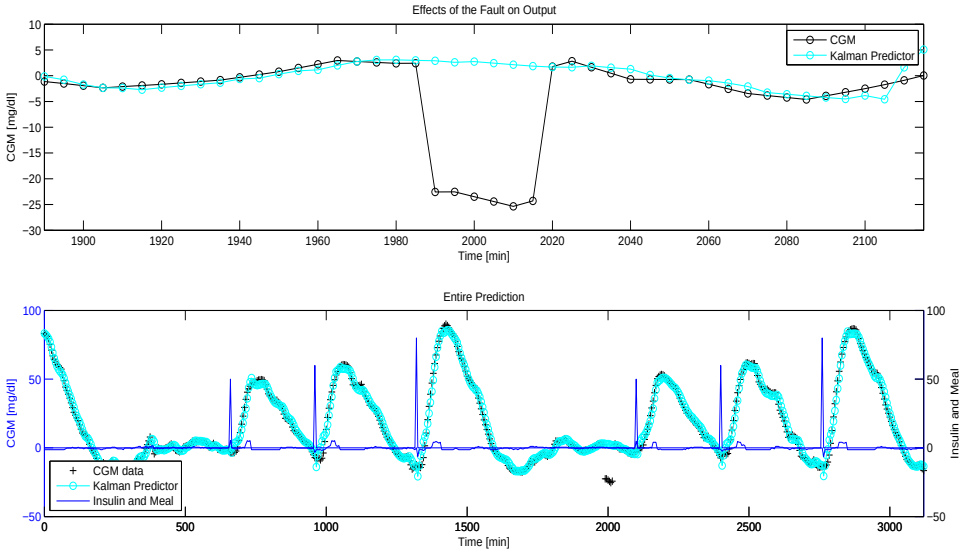

Figure 4.4: Prediction of Loss Failure.

4.3.2 Alarm 2 - Meal and Meal-Bolus

If the faults to be identified are the *meal fail* or the *meal-bolus fail* the Fault Detection Algorithm works in a different way. It always checks if the measurement falls outside the confidence interval of the 1-step on-line prediction, but it alarms only if this event happen for 3 consecutive times. Futhermore it must be that the 3 consecutive faulty samples, had all higher values or had all lower values than the measurements, see the scheme in Figure 4.8.
These modifications always allows to detect quickly the faults but also to classify the latter as caused by the meal event.
In Figure 4.5 and in Figure 4.6 can be seen the predictions of the algorithm respectively for the *meal fail* and the *meal-bolus fail*.

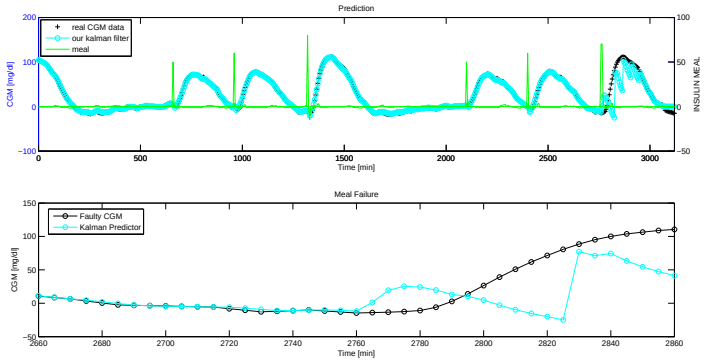

(a) Prediction Meal Faulty -100%

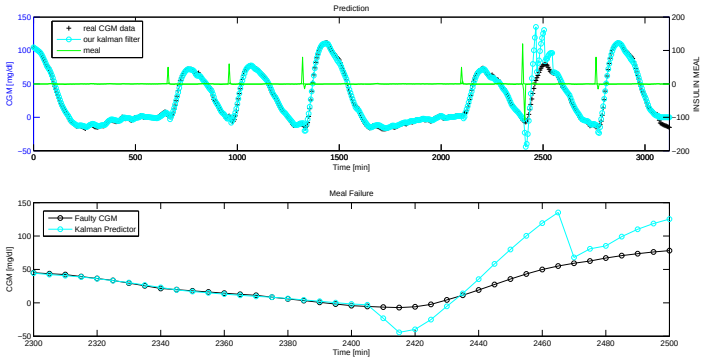

(b) Prediction Meal Faulty +100%

Figure 4.5: Prediction of Meal Failure.

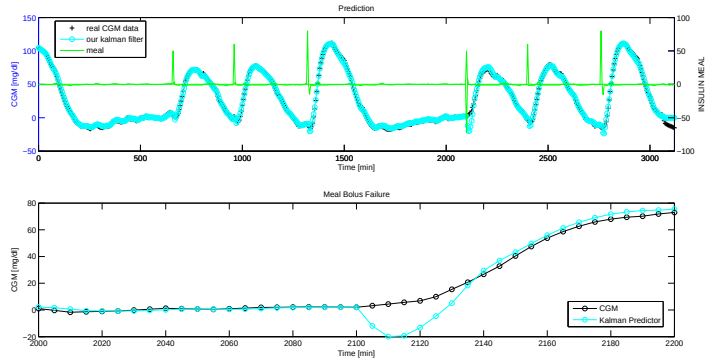

(a) Prediction Meal Bolus Faulty -100%

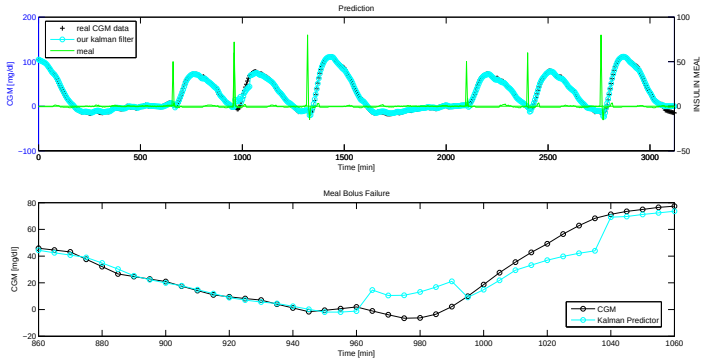

(b) Prediction Meal Bolus Faulty +100%

Figure 4.6: Prediction of meal-bolus failure.

4.3.3 Alarm 3 - Basal Failure

It is consider now the last type of simulated fault, the basal failure.
The insulin once injected, takes almost an hour before acting and to perceive its effect. Therefore it is reasonable to think that if the detection method is very accurate and moreover the amplitude of the fault is remarkable, it takes about two hours to notice that something is wrong.
If these conditions are less pronounced, it could takes a longer time, so it has become necessary to lengthen the predictive horizon, thus obtaining a lower reliability of the prediction, see Figure 4.2. Futhermore, this time the alert is given when for each $k = 3, ..., 12$, the CGM values fall outside the corresponding retrospective prediction with its confidence intervals. This fault is definitely the biggest challenge to deal.
In Figure 4.7 (a) and (b) can be seen the predictions of the algorithm for the faults

relative to a decrease of 50% and increase of 200% of the basal.

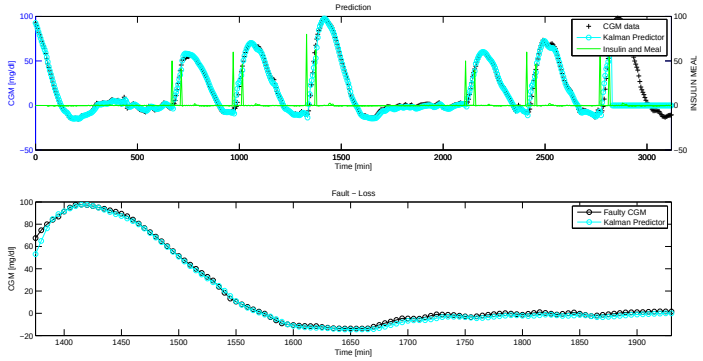

(a) Prediction Basal Faulty -50%

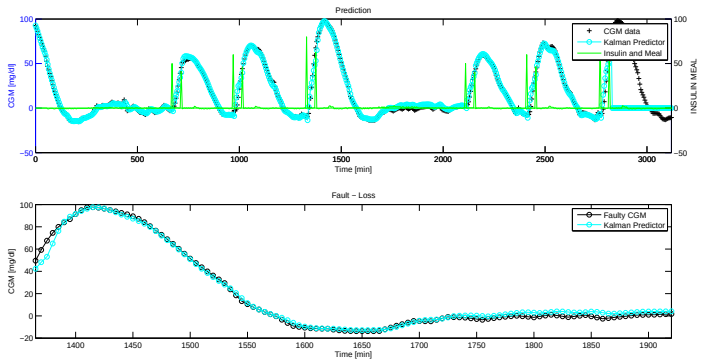

(b) Prediction Basal Faulty +200%

Figure 4.7: Prediction of Basal Failure

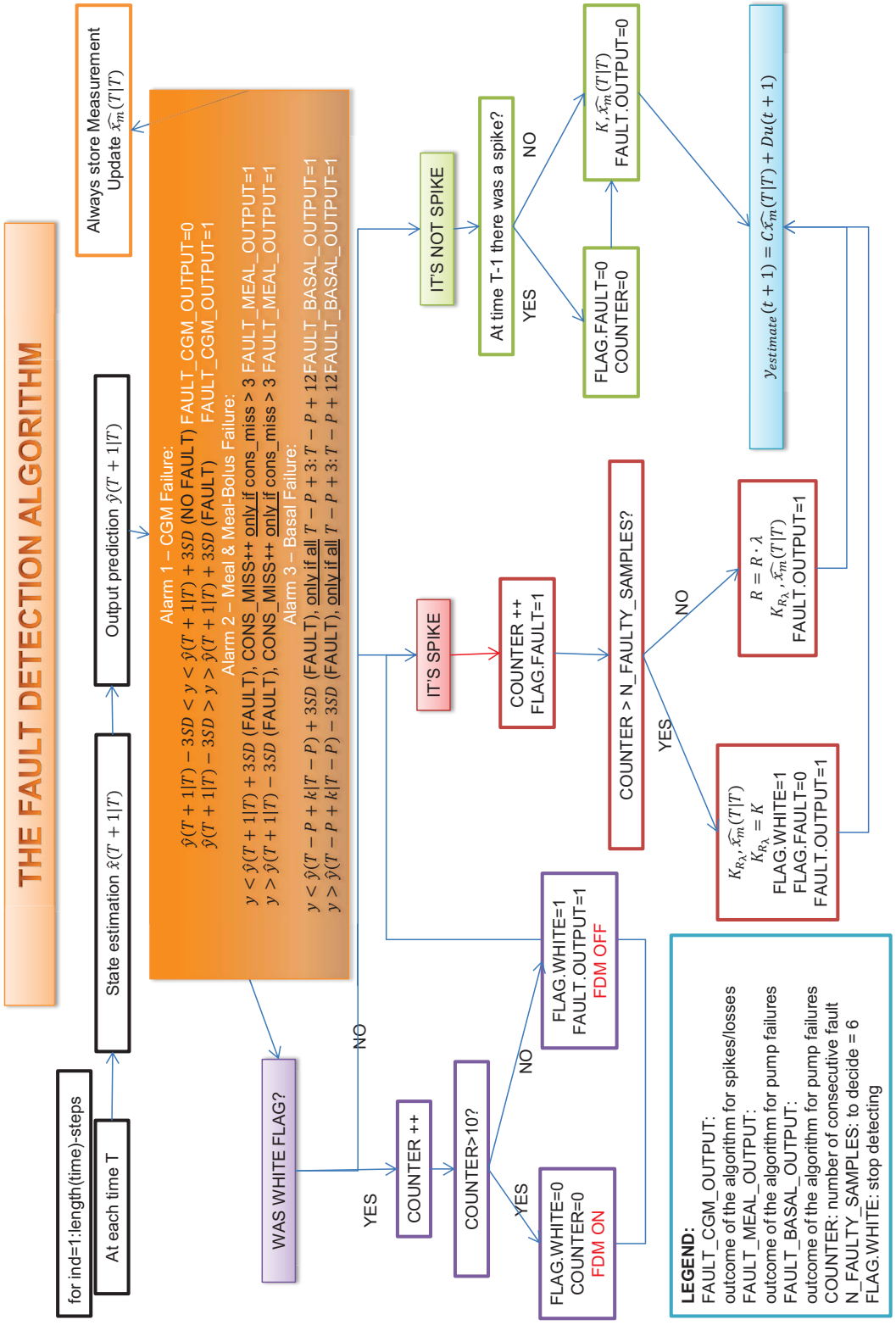

Figure 4.8: FDM

Chapter 5

Assessment of the method

The physiological simulator of a diabetic patient, developed by the University of Padova [9], allows to create different tracks with which it's possible to simulate the most various scenarios to test in a quickly and safety mode the new algorithms. Simulations are becoming crucial in this field, and being possible to incorporate any failures that affects the various devices, the robustness of the fault detection method can be tested.
In this chapter the 5 data-set used for the simulations are presented and the method of analysis on the different cases is shown.

5.1 Description of the data-set

The algorithm and analysis developed were done on in silico data obtained from the UVA/Padova Type-1 diabetic simulator [9]. Various scenarios were created:

- 100 virtual subjects with CGM failures spikes of different amplitudes and quantity;
- 100 virtual subjects with CGM failures compression artifacts of different amplitudes and durations;
- 100 virtual subjects with MEAL failures of different amplitudes;
- 100 virtual subjects with MEAL-BOLUS failures of different amplitudes;

- 100 virtual subjects with BASAL PUMP failures of different amplitudes and durations;

This simulator [9] was approved by the *US Food and Drug Administartion* as a substitute of animal testing, before starting the closed-loop clinical trials on humans. For each subject created, 6 days of closed loop control with 3 meals per day were simulated. The initial hour was midnight, the breakfasts, lunches and dinners occurred at 07:30, 13:00, and 19:30, respectively with charbohydrates consuption of 50 g, 60 g and 80 g.

5.1.1 Compression Artifacts - Spikes and Losses

Can now be explained how the failures were created, starting from the compression artifacts.
As was said in Chapter 2, can occur two realizations of this kind of failure which substantially differ in duration: one is the Spike the other one is the Loss.

The *spike* is an single glucose reading recepted by the CGM with an error rather greater than that normally. For simulating it, an anomalosly large measurement amplitude, $\mathbf{A} = -7.5, \quad -10, \quad -15, \quad -20, \quad -25, \quad mg/dl$, was added to the CGM measure at a random time t_{rand} so that:

$$CGM_{Faulty}(t_{rand}) = CGM_{noFaulty}(t_{rand}) + A$$

In Figure 5.1 a Spike is visible at $t = 2650min$ with an amplitude of $-25 \quad mg/dl$ and as can be seen, the value is not consistent with the past story and with the inputs nearby. The method implemented in this thesis, has the purpose of detected the spike and therefore to alarm in real time.

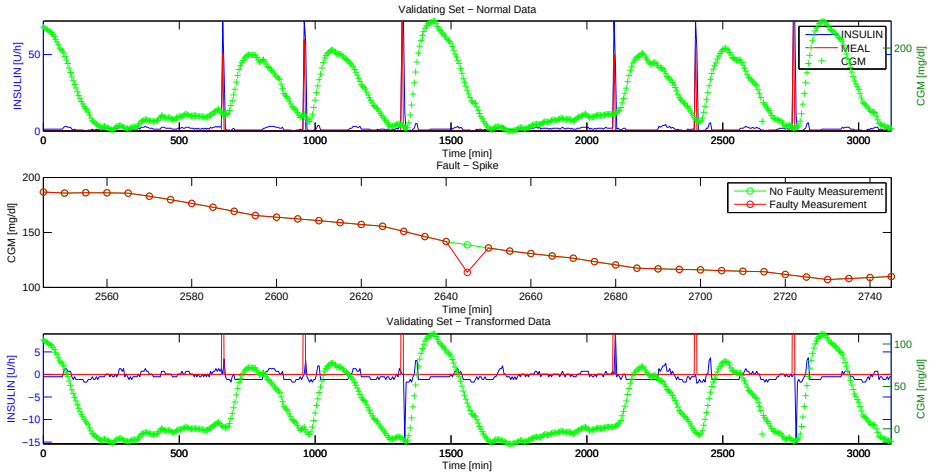

Figure 5.1: Insertion of a spike at t=2650 min.

The **transient loss of sensitivity** of the sensor, or simply loss, corresponds to a systematic underestimation of the glucose concentration for several consecutive samples. As for the spikes an anomalosly large measurement error of different amplitude, $\mathbf{A} = -7.5, \quad -10, \quad -15, \quad -20, \quad -25 \quad mg/dl$, was added to the CGM measure starting from a random time t_{rand} but in this case the error was propagated for some different durations: $\mathbf{D} = 10, \quad 20, \quad 30, \quad 60 \quad min$. It must be remembered that the sampling time of the CGM is $T_{samp} = 5 \quad min$.

$$CGM_{Faulty}(t_{rand} : t_{rand} + D) = CGM_{noFaulty}(t_{rand} : t_{rand} + D) + A$$

In Figure 5.2 a Loss starts at $t = 1220min$ and ends at $t = 1285 \quad min$ with an amplitude of $-25 \quad mg/dl$. Again, the values aren't consistent with the past story and with the inputs so this is a fault that must be catched by the FDM.

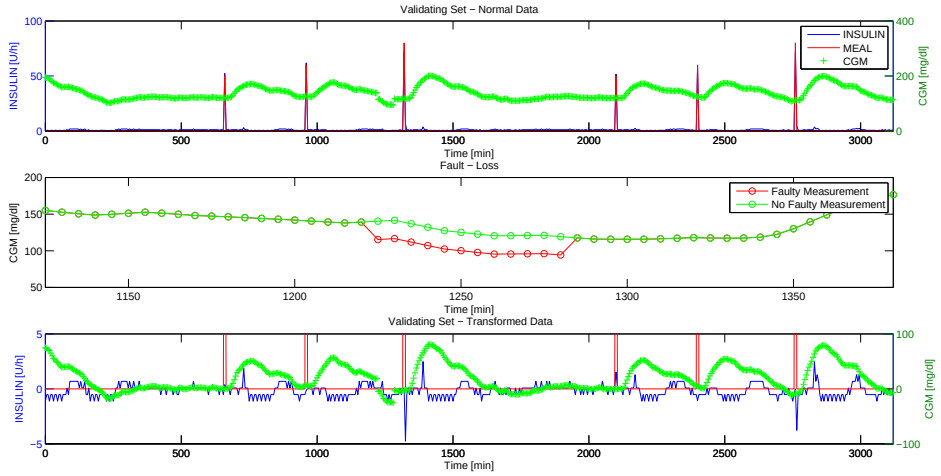

Figure 5.2: Insertion of a loss starting at t=1220 min

5.1.2 Meal Failure

To simulate this type of fault, it was decided to increase or decrease the amplitude of a random meal by a certain percentage. The values of the considered relative amplitudes used for the simulations were changed to: $\mathbf{E} = -100\%, \quad -75\%, \quad -50\%, \quad -25\%, \quad +25\%, \quad +50\%, \quad +75\%, \quad +100\%$:

$$Meal_{Faulty}(t_{randMeal}) = Meal_{noFaulty}(t_{randMeal})(1 + \frac{E}{100})$$

Figure 5.3 shows a miss announcement, $E = -100\%$:
Instead Figure 5.4 shows an announcement greater of the 100%, $E = +100\%$:

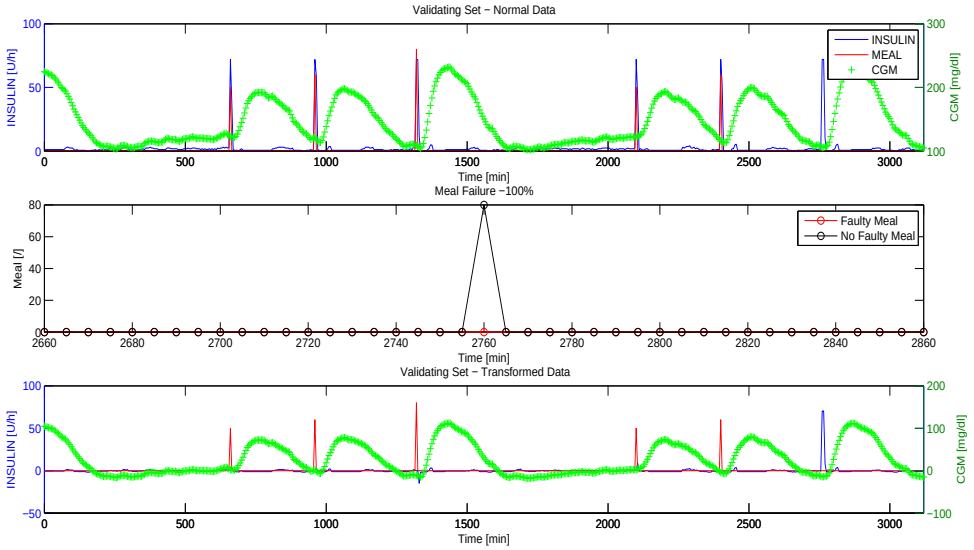

Figure 5.3: Miss meal announcement (-100%) at t=2760 min.

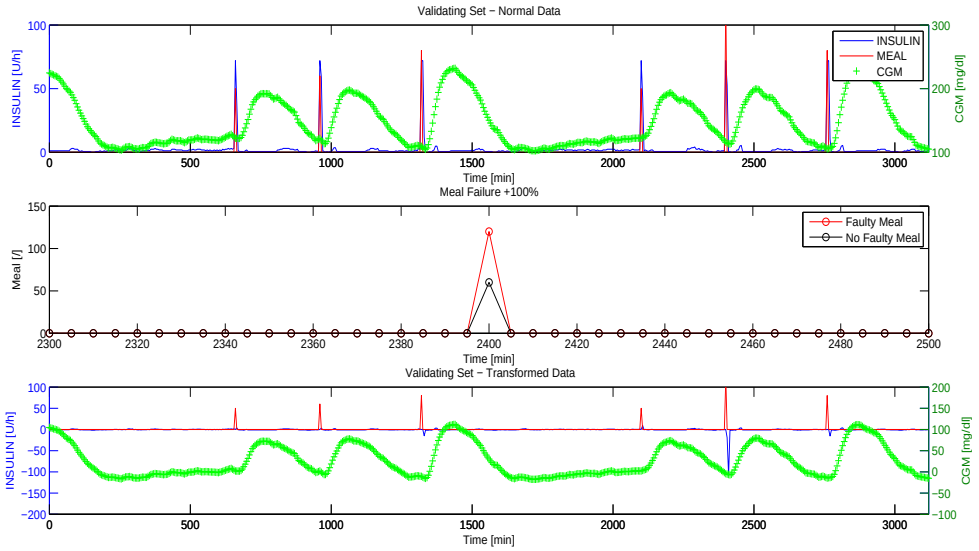

Figure 5.4: Wrong meal announcement (+100%) at t=2400 min.

5.1.3 Meal-Bolus Failure

The meal-bolus failure is a fault involving the insulin pump.
In Figure 5.5 there is one of the simulated cases for this kind of fault. At time $t = 2100min$ the insulin delivered, about 80 U/h, i.e. $\frac{80}{12} \approx 6.6U$, (the black line) doesn't appear to the system that believed to has received only about 40 U/h (the red line).

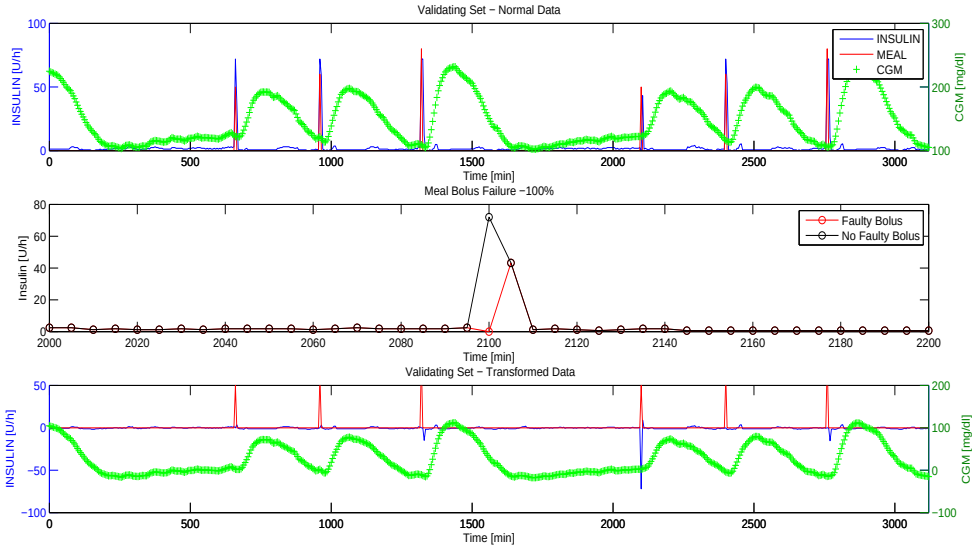

Figure 5.5: Communication error on meal-bolus (-100%) at t=2100 min.

In Figure 5.6 there is another case. In this scenario the AP received an higher information on the quantity of insulin delivered. At time $t = 960$ min the insulin was about 60 U/h (black line) but for some reason, it results to the system that the insulin delivered was about 150 U/h (red line). With this information the DiAs estimates in a wrong way the future profile, giving in particular less insulin than it should.

Also to simulate this type of fault, it was decided to increase or decrease the amplitude of a random insulin bolus by a certain percentage. The values of the considered relative amplitudes used for the simulations were still changed to: $\mathbf{E} = -100\%, \quad -75\%, \quad -50\%, \quad -25\%, \quad +25\%, \quad +50\%, \quad +75\%, \quad +100\%$:

$$Insulin_{Faulty}(t_{randBolus}) = Insulin_{noFaulty}(t_{randBolus})(1 + \frac{E}{100})$$

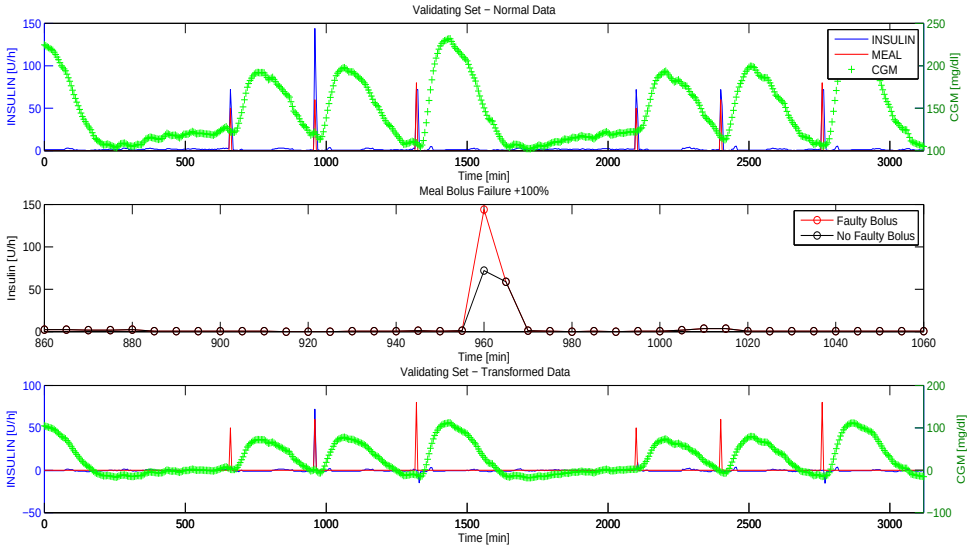

Figure 5.6: Wrong meal-bolus amount (+100%) at t=960 min.

5.1.4 Basal Failures

To simulate this fault, it was decided to decrease or increase the amplitude of a random portion of basal insulin (making attention to don't include any bolus) by a certain percentage. Thus, in addition to the increase or decrease of the amplitudes, different durations were used too: $\mathbf{E} = -100\%, \quad -50\%, \quad +50\%, \quad +100$, $\mathbf{D} = 1, \quad 2, \quad 3, \quad 4, \quad 6$ hours.

$$Insulin_{Faulty}(t_{rand} : t_{rand} + D) = Insulin_{noFaulty}(t_{rand} : t_{rand} + D)(1 + \frac{E}{100})$$

In Figure 5.7, it can be seen one of the possible cases which were described above.

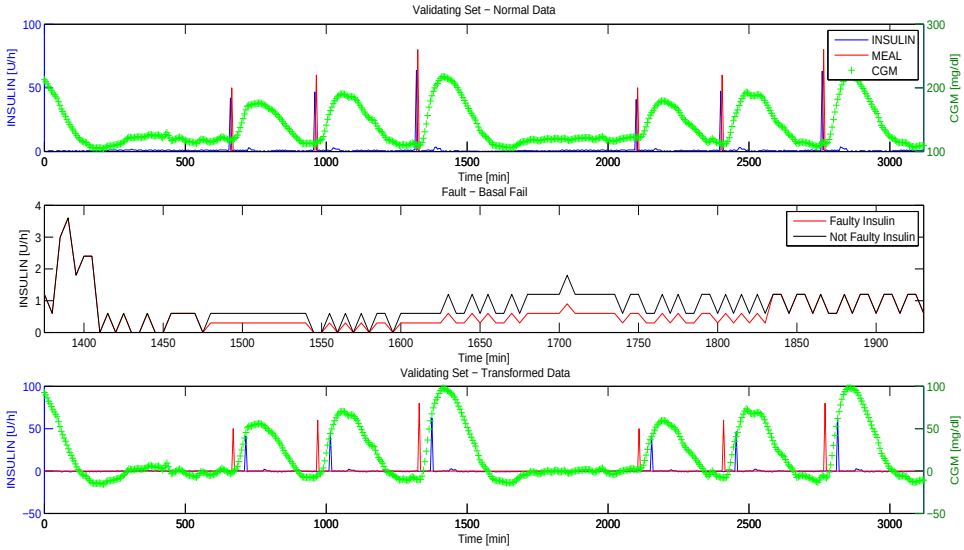

Figure 5.7: Decrease of the basal insulin (-50%) for 6 hours.

Another unlucky possibility, is the one that can be seen in Figure 5.8. The basal insulin is higher than what is expected and this situation can verify if there are some technological issues, especially during the testing of new insulin pump that can require different settings from others to work in the right way, or if the patient informations that were inserted to the DiAs at the starting of the session were wrong.

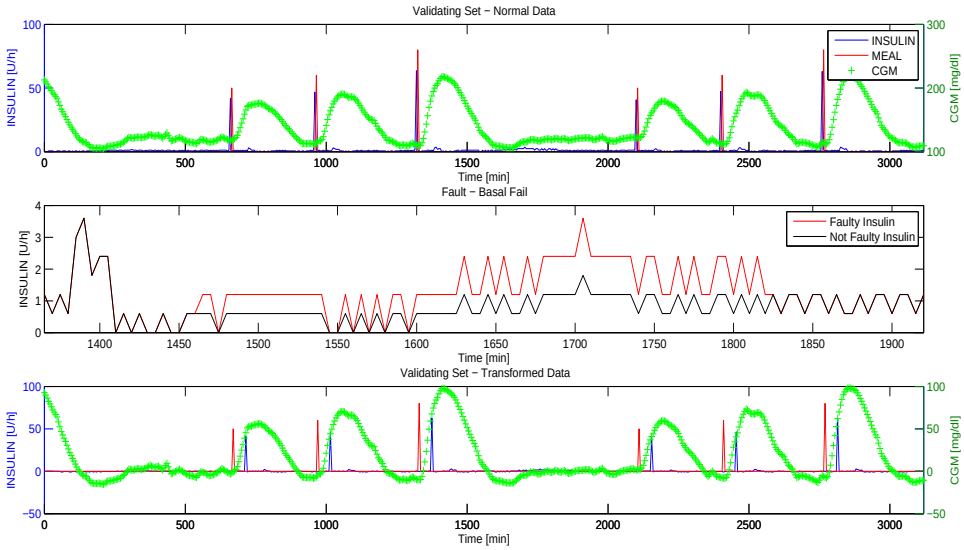

Figure 5.8: Increase of the basal insulin (+200%) for 6 hours.

5.2 Statistical Analysis

One of the main aims of this study is to define how effective is the method in detecting faults, how many times it returns false alarms and how many times it doesn't notice the presence of the fault.
In order to quantify the results obtained, suitable indices must be introduced to take into account different statistical aspects. Moreover these indices must be drawn from appropriate observation intervals; thus, becomes essential to define how long the signals must be observed before to classify a portion of their.

5.2.1 Compression Artifacts - Spikes and Losses

First of all, consider the compression artifacts and assume that for this class of faults, the length of the observation interval is as long as the fault length.
Thus for example, for a single spike the length of the observation interval is 1 sample instead for a loss with a duration of 1 hour, the length of observation interval is 12 samples.
Considering now the CGM signal and the classifier described above, there are 4 possible outcomes:

1. **True Positive (TP)**: if the samples are faulty and they are identified by the algorithm as faulty *(Positive Outcome)*;
2. **True Negative (TN)**: if the samples are not faulty and they are not identified by the algorithm as faulty *(Negative Outcome)*;
3. **False Negative (FN)**: if the samples are faulty and they are not identified by the algorithm as faulty *(Negative Outcome)*;
4. **False Positive (FP)**: if the samples are not faulty but they are identified by the algorithm as faulty *(Positive Outcome)*.

An easy example that illustrates the previous definitions for the spike fault, is reported in the following table:
Note that, with regard to the loss fault, it makes sense to consider as TP also a partial detection, so if at least one of the faulty samples within the range of observation, is detected as faulty it can be said that the algorithm identified the loss.

0	0	0	0	1	1	1	1	1	1	0	0	0	1	0	1	1	1	1	1
0	0	0	0	0	0	0	0	0	0	1	1	1	1	1	1	1	1	1	1
TN	TN	TN	TN	FN	FN	FN	FN	FN	FN	FP	FP	FP	TP	FP	TP	TP	TP	TP	TP

Figure 5.9: **I row**: real signal; **II row**: outcome of the algorithm; **III row**: associated index.

In Figure 5.10 it's reported a two-by-two *confusion matrix* from which can be derived many important and common indices, useful for the subsequent analysis:

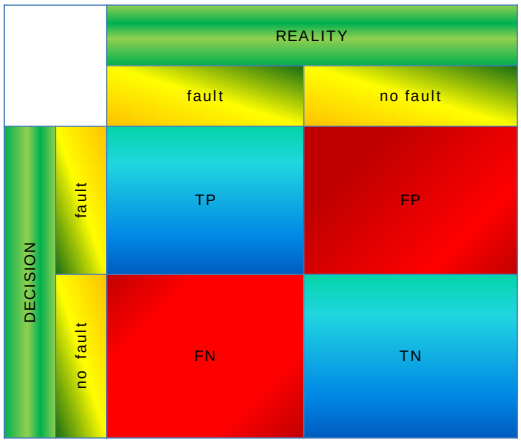

Figure 5.10: Table describing the relationships among terms.

The True Positive index and the True Negative index located in the diagonal, rapresent the correct decision made by the alghoritm; instead, in the other diagonal, the True Negative index and the False Negative index represent the errors committed. Considering the first column of the matrix, can be derived the total number of faulty samples that were present in the signal as:

$$\text{Number of Events} = TP + FN \tag{5.1}$$

Considering the first and second rows of the matrix, two indeces can be derived respectively accounting for the percentage of alarms that are properly identified as fault and the percentage of *no-alarms* corresponding to when correctly nothing is reported:

$$PPV = \frac{TP}{TP+FP} \quad \text{Positive Predictive Value}$$
$$NPV = \frac{TN}{TN+FN} \quad \text{Negative Predictive Value} \tag{5.2}$$

Considering the first and second columns of the matrix, two indeces can be derived respectively relating the algorithm ability to rightly identify a sample when it's faulty and to rightly identify a sample when it's not faulty.

$$\text{TPR} = \frac{TP}{TP+FN} \quad \text{Sensitivity}$$
$$\text{TNR} = \frac{TN}{TN+FP} \quad \text{Specificity} \tag{5.3}$$

Finally an index that relates to the proportion of true results compared to all classifications:

$$\text{Accuracy} = \frac{TP+TN}{TP+TN+FP+FN} \tag{5.4}$$

5.2.2 Meal and Meal-Bolus Failures

Consider now the *meal failure* and the *meal-bolus failure*. Because of the slower dynamics than the previous faults, it is necessary to wait more time to see some changes in the CGM track. For this reason the observation interval was stretched to 4 hours and the following indices were re-defined as:

1. **True Positive (TP)**: if into the observation interval, there is a faulty sample and it is identify by the algorithm although with some delay *(Positive Outcome)*;

2. **True Negative (TN)**: if all the samples into the observation interval are not faulty and they are not identified by the algorithm as faulty *(Negative Outcome)*;

3. **False Negative (FN)**: if into the observation interval, there is a faulty sample and it's not identify by the algorithm as faulty *(Negative Outcome)*;

4. **False Positive (FP)**: if into the observation interval, the samples are not faulty but they are identified by the algorithm as faulty *(Positive Outcome)*.

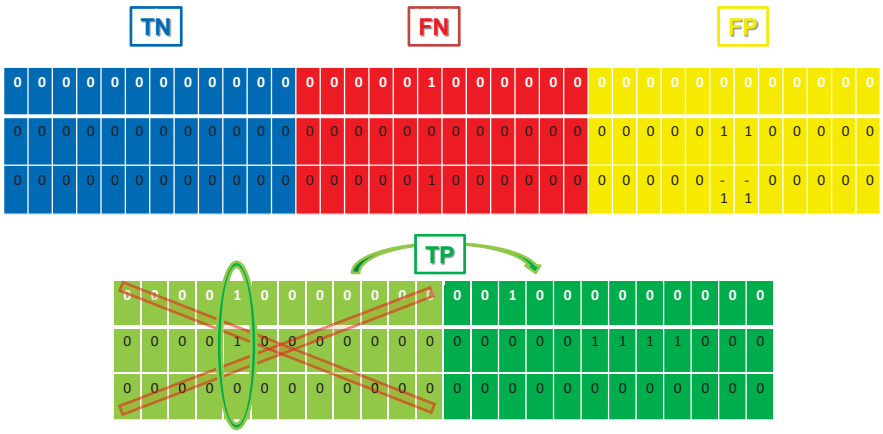

Figure 5.11: Redefinition of the indeces: TN,FN,FP,TP.

To aid understanding, the above definitions are summarized in Figure 5.11:
Once obtained these the 4 indices as well redefined, the others coming from the *confusion matrix* can be calculated as described previously.

5.2.3 Basal Failure

The last definitions of TP, TN, FN, and FP that were used for the meal and meal - bolus failures can be also used for the basal failure. At difference with the previous case, however, the observation interval that was imposed equal to 6 hours, because of the slowest dynamic previously described.

Chapter 6

Results with Simulated Data

6.1 The choise of the amplitude of the confidence interval: the ROC analysis

A receiver operating characteristics (ROC) curve is a technique [10] for visualizing, organizing and selecting classifiers based on their performance.
This method allows obtaining a particular chart, called *ROC graph*, which is two-dimensional and has on the $X - axis$ the False Positive Rate, $FPR = 100 -$ Specificity, and on the $Y - axis$ the True Positive Rate, $TPR =$ Sensitivity. Thus, each point of the ROC curve represents a sensitivity/specificity pair corresponding to a particular decision threshold.
In case of the Failure Detection Method, the technique depicts relative tradeoffs between TP and FP in function of the parameter m, which represents the number of SD considered for the confidence interval, (see equation **??** of Chapter 4).
The aim of the analysis is to identify the value of m that allows getting the best performance, taking into account the trade off given by succeeding in detecting correctly the failures and not producing an excessive amount of false alarms.
There are some important points to highlight in the ROC space:

- the lower left point $(0, 0)$ represents the strategy of never issuing a positive classification, so there are not FP but also not TP;
- the upper right point $(100, 100)$ represents the strategy of always issuing a positive classification, so there are a lot of TP but also a lot of FP;

- the upper left point $(0, 100)$, representing 100% of sensitivity (there are not FN) and 100% of specificity (there are not FP), which is the perfect classification;
- the points on the diagonal $x = y$, are usually defined as *random guesses* [10]. This means that if a classifier randomly guesses the positive class the 70% of the time, it can be expected to get the 70% of positives (P = TP + FN) correct but at the same time, its false positive rate will increase to 70%, yielding (70 ; 70) in the ROC space.

Thus, to get a satisfactory result, the value of the parameter m that is closer to the upper left point, must be chosen.

The candidate values for m, starts from 2 with a step of 0.1 up to 4.
For the choice of the optimal m value, three different scenarios of failures on CGM signals were used:

- Scenario 1: only 1 spike for each subject;
- Scenario 2: 5 random spikes for each subject;
- Scenario 3: only 1 loss for each subject;

For each of the scenarios reported, different amplitudes of the compression artifacts were considered, spanning from $5mg/dl$ to $25mg/dl$.
The Table 6.1 shows the results for Scenario 1. Focusing on it would seem that $m = 2.1$ might be the best choice, beacuse it corresponds to the higher number of best pairs sensitivity/specificity compared to the other values.
Refering now on Table 6.2, it seems that a value slightly higher for m, such as $m = 2.4$, would be the right choice for the Scenario 2.
However in the case of this study, it is more important to identify the most dangerous faults, which are definitely those with the higher amplitudes.
So considering also the Tables 6.3, which refers to Scenario 3, it can be seen that in case of higher amplitudes, i.e. 20 and $25mg/dL$, the best choice for the parameter is $m = 3$.
Even considering the Euclidean distance from the point of perfect classification and the best pair sensitivity/specificity for each amplitude, see Tables 6.4, it results that

until $8mg/dL$, the best choice would be $m = 2.1$. Again moving to larger amplitudes, which are most significant for the aim of fault detection, the most appropriate value is $m = 3$.

Finally, in Figures 6.1, 6.2 and 6.3 can be seen the resulting ROC graph respectively of the Scenario 1, 2 and 3. It is to note that the scale is not uniform, but the plots are the zooms of interest areas. Each point corresponds to a hypothesized value of m and can be seen how all the points starting from 2.1 till 3.2 have similar sensitivity/specificity pair. Nevertheless, $m = 3$ has in all the three scenarios, the best sensitivity values.

On the basis of these considerations and on the really positive results which were obtained in detections of the most relevant failures, $m = 3$ was choosen.

Of note, m=3, guarantees good performance also in case of low fault amplitudes.

	5 mg/dL		6 mg/dL		7 mg/dL		8 mg/dL		9 mg/dL		10 mg/dL	
	SNS	SPC	SNS	SPC	SNS	SPC	SNS	SPC	SNS	SPC	SNS	SPC
2	66	91	79	79	87	91	97	92	98	91.9	98	91.9
2.1	64	92.8	74	74	86	93.3	96	93.7	98	93.7	98	93.7
2.2	62	94	74	74	85	94.4	93	94.7	98	94.8	98	94.8
2.3	60	94.9	72	72	85	95.3	90	95.5	98	95.8	98	95.8
2.4	57	95.5	69	69	81	95.9	89	96.2	97	96.4	98	96.4
2.5	51	96.3	68	68	77	96.6	86	96.9	95	97.2	98	97.3
2.6	47	97.2	62	62	74	97.4	85	97.7	92	97.9	98	98.1
2.7	43	98	62	62	73	98	85	98.3	91	98.4	98	98.7
2.8	41	98	60	60	72	98.4	83	98.6	90	98.8	97	99
2.9	38	98.7	56	56	70	98.6	80	98.7	88	98.9	96	99.2
3	36	98.9	52	52	67	98.7	76	98.8	87	99.1	93	99.3
3.1	33	99.1	51	51	64	98.9	75	99	85	99.2	92	99.4
3.2	30	99.3	45	45	61	98.9	74	99.1	83	99.2	92	99.5
3.3	27	99.4	44	44	59	99.2	73	99.3	81	99.3	89	99.5
3.4	24	99.5	42	42	58	99.3	69	99.2	79	99.4	88	99.6
3.5	22	99.6	38	38	53	99.3	67	99.2	77	99.3	84	99.4
3.6	19	99.7	35	35	51	99.3	64	99.3	75	99.3	83	99.4
3.7	17	99.7	31	31	48	99.3	59	99.3	73	99.3	82	99.5
3.8	17	99.7	27	27	44	99.3	59	99.3	72	99.3	80	99.4
3.9	14	99.8	24	24	42	99.4	56	99.4	68	99.3	79	99.5
4	12	99.6	22	22	40	99.4	54	99.4	67	99.3	78	99.5

Table 6.1: Sensitivity and Specificity pair for data-set with 1 spike of $5, 6, 7, 8, 9, 10 mg/dL$ amplitude.

	5 mg/dL		6 mg/dL		7 mg/dL		8 mg/dL		9 mg/dL		10 mg/dL	
	SNS	SPC	SNS	SPC	SNS	SPC	SNS	SPC	SNS	SPC	SNS	SPC
2	65.7	89.1	76.3	89.3	86.2	90.3	89.9	90.8	91	91.1	92.7	91.3
2.1	64.3	90.9	74.6	90.8	85.8	91.9	90.3	92.6	91.8	92.8	92.9	92.9
2.2	60	91.6	72.6	91.7	82.7	92.6	88.7	93.5	91.6	93.7	92.7	94.1
2.3	57.1	92.8	70.6	92.6	80.9	93.4	87.5	94.3	91	94.7	92.3	94.8
2.4	53.7	93.4	67.9	93.4	79.9	94.1	86.7	94.9	91	95.3	91.9	95.6
2.5	51	94.2	64.6	94	78	94.9	83.8	95.3	89.8	95.9	92.1	96.3
2.6	47.6	94.9	62.2	94.6	74.6	95.4	82.8	96	89.4	96.6	91.3	97
2.7	43.9	95.7	60.5	95.3	71.5	95.8	80.4	96.2	89.2	97.2	91.1	97.5
2.8	41.6	96.1	56.9	95.7	67.7	95.9	78.4	96.5	87.8	97.4	90.9	97.8
2.9	37.3	96.5	53	96.1	64.4	96	75.4	96.5	86.9	97.6	90.3	98
3	33.3	97	50.9	96.5	61.6	96.1	73.1	96.6	85.1	97.5	89.7	98.1
3.1	29.2	97.2	45.6	96.6	58.3	96.2	70.3	96.7	84.3	97.7	88	98.2
3.2	26.5	97.4	41.9	96.9	53.7	96.2	68.5	96.7	82.2	97.6	87.2	98.2
3.3	23.5	97.7	38.9	97.1	49.2	96.1	66.9	96.8	80.2	97.6	86.6	98.2
3.4	21.2	98	35.8	97.2	45.7	96.1	64	96.9	78.6	97.6	84.8	98.2
3.5	18.4	98.3	33.3	97.6	43.9	96.2	61.6	96.9	76.5	97.5	82.8	97.9
3.6	15.9	98.5	30.7	97.8	42.1	96.4	58.2	96.9	73.5	97.4	80.5	97.8
3.7	13.5	98.5	28.8	97.9	40	96.6	54.7	96.8	71.2	97.3	79.9	97.9
3.8	12.2	98.8	26.2	98	36.6	96.7	51.9	96.7	68.6	97.1	78.1	97.8
3.9	10	98.9	23.3	98.1	33.9	96.8	49.3	96.8	65.1	97	75.9	97.8
4	8.8	99.1	20.9	98.3	31.9	97.1	45.7	96.8	62.7	97	74.6	97.7

Table 6.2: Sensitivity and Specificity pair for data-set with 5 spikes of $5, 6, 7, 8, 9, 10 mg/dL$ amplitude.

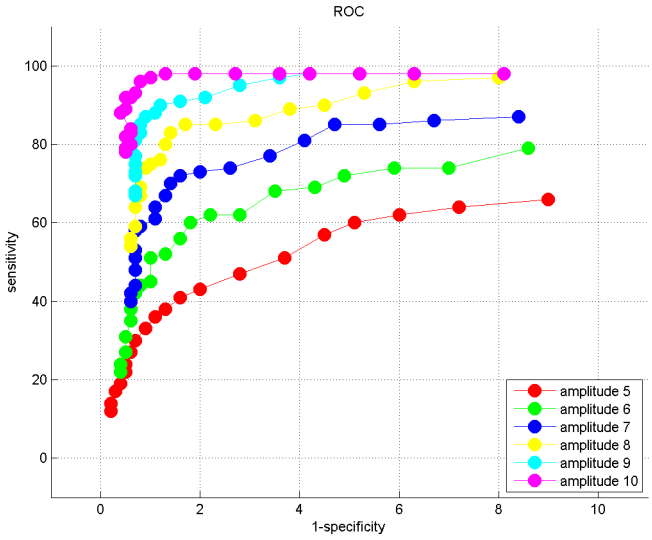

Figure 6.1: Zoom of ROC graph for Scenario 1. The amplitudes of the spike are: $5, 6, 7, 8, 9, 10 mg/dL$.

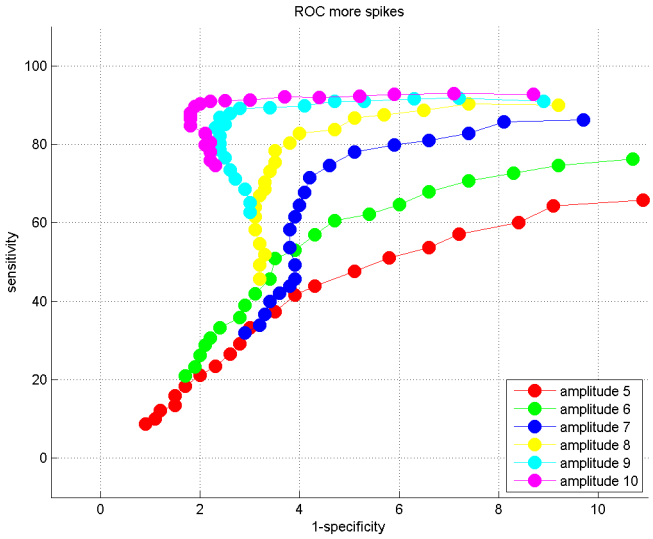

Figure 6.2: Zoom of ROC graph for Scenario 2. The amplitudes of the spikes are: $5, 6, 7, 8, 9, 10 mg/dL$ amplitude.

	5 mg/dL		6 mg/dL		7 mg/dL		8 mg/dL		9 mg/dL		10 mg/dL		15 mg/dL		20 mg/dL		25 mg/dL	
	SNS	SPC	SNS	SPC	SNS	SPC	SNS	SPC	SNS	SPC	SNS	SPC	SNS	SPC	SNS	SPC	SNS	SPC
2	44.8	90.7	59.3	90.6	71.3	90.8	75.5	90.7	79.8	90.6	86	90.7	94.5	91.2	97.3	91.4	98	91.5
2.1	40	92.6	55.5	92.4	67	92.4	73.3	92.5	76.8	92.3	81.3	92.3	93	92.8	97	93.1	97.8	93.2
2.2	37.5	94.2	51.7	93.9	61	93.8	71.3	94	76	93.9	79.5	93.7	91.8	94	96.5	94.5	97.8	94.6
2.3	33.8	95.4	46	95.1	57.3	94.8	67.8	95	73.8	94.9	77.8	94.9	90.8	95.1	95.8	95.5	97.8	95.7
2.4	30.8	96.3	40	96	54.5	95.8	65.8	95.8	70.3	95.9	76	95.8	90	95.9	95.8	96.4	97.8	96.6
2.5	30	97.2	39	96.9	50	96.7	58.8	96.4	68	96.7	73.8	96.6	88.8	96.6	95.5	97.1	97.3	97.3
2.6	26.8	97.7	36.3	97.5	46.8	97.3	56.5	97.1	65.8	97.2	71.8	97.2	87	97	94.8	97.6	97	97.9
2.7	24.5	98.2	34	97.9	43.8	97.7	53	97.5	62.5	97.4	68	97.5	85.3	97.6	93.5	97.8	96.5	98.1
2.8	21	98.5	31.3	98.2	40.3	98	49.8	97.8	58.5	97.6	65.8	97.7	83.8	97.6	92.3	98	96.3	98.3
2.9	19.3	98.8	29.8	98.6	38	98.3	46.8	98.1	54.8	97.9	63	97.9	81.8	97.8	91.3	98.1	96	98.6
3	16.8	99.1	27.3	98.8	35.3	98.5	45.3	98.3	51.7	98.2	60.8	98.2	81	98.1	90.5	98.1	95.5	98.7
3.1	14.5	99.3	24.5	99.1	33.5	98.8	42	98.6	49.5	98.4	57	98.3	78.3	98.1	89	98.3	95.3	98.9
3.2	12	99.4	21.8	99.3	31.5	99	40.3	98.8	47.8	98.6	54	98.4	78.3	98.3	88	98.4	94.5	98.9
3.3	10.3	99.6	19.5	99.4	29.3	99.2	37.5	98.9	46	98.8	51.2	98.6	76.5	98.5	87.3	98.4	93.3	98.9
3.4	9	99.7	17.8	99.5	27.5	99.3	34	99	44	98.8	48.8	98.7	75.3	98.6	85.8	98.5	92.8	98.8
3.5	7.8	99.7	16.3	99.5	25	99.4	32	99.1	42	98.9	48.5	98.8	73.8	98.7	83.8	98.5	91.8	98.8
3.6	7.5	99.8	14.5	99.6	21.5	99.4	30.8	99.2	39.5	98.9	46.3	98.9	73	98.7	82.8	98.6	90.5	98.7
3.7	7.2	99.8	12.5	99.6	19.5	99.5	29	99.3	37.3	99	44.5	98.9	71	98.8	81.5	98.6	89.8	98.7
3.8	6	99.9	11.3	99.7	18.3	99.5	27.8	99.3	33.3	99.1	43.5	98.9	69.3	98.8	80.8	98.6	88.8	98.6
3.9	5.3	99.9	9.5	99.8	16.5	99.6	25	99.5	31	99.2	40.5	99	67	98.7	79.3	98.6	87.8	98.5
4	4.5	99.9	8	99.9	16	99.7	22.8	99.5	30.3	99.3	38.3	99.1	63.7	98.8	78.3	98.6	87.5	98.6

Table 6.3: Sensitivity and Specificity pair for data-set with 1 loss of $5, 6, 7, 8 mg/dL$ amplitude.

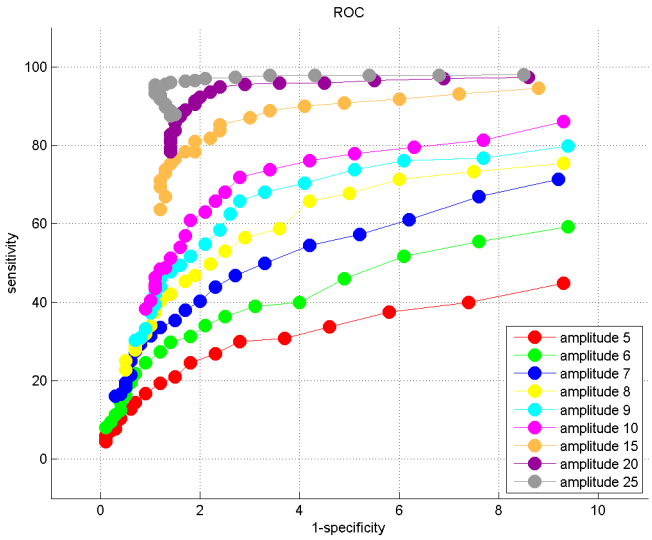

Figure 6.3: Zoom of ROC graph for data-set with with 1 loss of $5, 6, 7, 8, 9, 10, 15, 20, 25 mg/dL$ amplitude.

	Distance (spike)						Distance (loss)									Distance (more spikes)					
	5	6	7	8	9	10	5	6	7	8	9	10	5	6	7	8	9	10	15	20	25
2	35.2	22.7	15.5	8.5	8.3	8.3	36	26	16.9	13.7	12.7	11.4	56	41.8	30.1	26.2	22.3	16.8	10.4	9	8.7
2.1	36.7	26.9	15.5	7.5	6.6	6.6	36.8	27	16.3	12.2	10.9	10	60.5	45.1	33.9	27.7	24.4	20.2	10	7.5	7.1
2.2	38.5	26.7	16	8.8	5.6	5.6	40.9	28.6	18.8	13	10.5	9.4	62.8	48.7	39.5	29.3	24.8	21.4	10.2	6.5	5.8
2.3	40.3	28.4	15.7	11	4.7	4.7	43.5	30.3	20.2	13.7	10.4	9.3	66.4	54.2	43	32.6	26.7	22.8	10.4	6.2	4.8
2.4	43.2	31.3	19.4	11.6	4.7	4.1	46.8	32.8	20.9	14.2	10.2	9.2	69.3	60.1	45.7	34.5	30	24.4	10.8	5.5	4
2.5	49.1	32.2	23.2	14.3	5.7	3.4	49.3	35.9	22.6	16.9	11	8.7	70.1	61.1	50.1	41.4	32.2	26.4	11.7	5.4	3.8
2.6	53.1	38.1	26.1	15.2	8.3	2.8	52.6	38.2	25.8	17.7	11.1	9.2	73.2	63.7	53.3	43.6	34.3	28.3	13.3	5.7	3.7
2.7	57	38.1	27.1	15.1	9.1	2.4	56.3	39.8	28.8	20	11.2	9.2	75.5	66	56.2	47.1	37.6	32.1	14.9	6.9	4
2.8	59	40	28	17.1	10.1	3.2	58.5	43.3	32.6	21.9	12.5	9.4	79	68.7	59.7	50.2	41.6	34.3	16.4	8	4.1
2.9	62	44	30	20	12.1	4.1	62.8	47.2	35.8	24.8	13.3	9.9	80.7	70.2	62	53.2	45.2	37.1	18.3	8.9	4.2
3	64	48	33	24	13	7	66.8	49.2	38.6	27.1	15.1	10.5	83.2	72.7	64.7	54.7	48.3	39.2	19.1	9.7	4.7
3.1	67	49	36	25	15	8	70.9	54.5	41.9	29.9	15.9	12.1	85.5	75.5	66.5	58	50.5	43	21.8	11.1	4.8
3.2	70	55	39	26	17	8	73.5	58.2	46.5	31.7	18	12.9	87.2	78.2	68.5	59.7	52.2	46	21.8	12.1	5.6
3.3	73	56	41	27	19	11	76.5	61.2	50.9	33.3	19.9	13.5	89.7	80.5	70.7	62.5	54	48.8	23.5	12.8	6.8
3.4	76	58	42	31	21	12	78.8	64.3	54.4	36.1	21.5	15.3	91	82.2	72.5	66	56	51.2	24.7	14.3	7.3
3.5	78	62	47	33	23	16	81.6	66.7	56.2	38.5	23.6	17.3	92.2	83.7	75	68	58	51.5	26.2	16.3	8.3
3.6	81	65	49	36	25	17	84.1	69.3	58	41.9	26.6	19.6	92.5	85.5	78.5	69.2	60.5	53.7	27	17.3	9.6
3.7	83	69	52	41	27	18	86.5	71.2	60.1	45.4	28.9	20.2	92.8	87.5	80.5	71	62.7	55.5	29	18.6	10.3
3.8	83	73	56	41	28	20	87.8	73.8	63.5	48.2	31.5	22	94	88.7	81.7	72.2	66.7	56.5	30.7	19.3	11.3
3.9	86	76	58	44	32	21	90	76.7	66.2	50.8	35	24.2	94.7	90.5	83.5	75	69	59.5	33	20.7	12.3
4	88	78	60	46	33	22	95.5	91.2	79.1	68.2	54.4	37.4	25.5	92	84	77.2	69.7	61.7	36.3	21.7	12.6

Table 6.4: Distance from the (0,100) point, data-set with 1 spike.

6.2 The Result Analysis

As anticipated in the previous chapter, the length of the observation interval is critical for a correct detection of the failures. As a consequence this parameter has been set to different values for different type of failures.
To be more specific, it is used a direct comparison when the compression artifacts were analyzed, an observation interval of 30 minutes for the meal failure, of 4 hours for the meal-bolus failure and of 6 hours for the basal failure.
These decisions come from the considerations reported in Chapter 2, on the dynamic effects of the differents kind of faults.
It follows the pseudo-code for the calculation of the indices explained in chapter 5, in particular the TN, FN, FP, TP with which it can be then calculated all the others:

```
if 'MealFail' then
 |   int_samp = 5;  ⇒ 30min
 else if 'BolusMealFail' then
 |   int_samp = 47;  ⇒ 4hours
 else if 'BasalFail' then
 |   int_samp = 71;  ⇒ 6hours
 else
 |   if 'Spike' then
 |    |   int_samp = 1;  ⇒ 5min
 |   else
 |    |   int_samp = d;  ⇒ D = [d_1, ..., d_N],   loss   duration
 |   end
 |
end
ind_Start ← FirstInd_RealFault;
ind_End ← ind_Start + int_samp;
while ind_End < length(Time) do
 |   if VectFDM(ind_Start : ind_End) == 0 ∧ VectRealFault(ind_Start : ind_End) == 0 then
 |    |   TN = TN + 1;
 |    else if VectFDM(ind_Start : ind_End) == 0 ∧ any(VectRealFault(ind_Start : ind_End)) == 1 then
 |    |   FN = FN + 1;
 |    else if VectRealFault(ind_Start : ind_End) == 0 ∧ any(VectFDM(ind_Start : ind_End)) == 1 then
 |    |   FP = FP + 1;
 |    else
 |    |   TP = TP + 1;
 |   end
 |   ind_Start ← ind_End + 1;
 |   ind_End ← ind_End + int_samp + 1;
end
ind_Start ← FirstInd_RealFault − int_samp − 1;
ind_End ← FirstInd_RealFault − 1;
while ind_End < length(Time) do
 |   ...
 |   ind_End ← ind_Start − 1;
 |   ind_Start ← ind_End − int_samp;
end
```

It is important to note that for each type of failure, the observation interval starts

exactly from the first index of the real fault. For example, if the basal failure starts at time t_1 and ends at time t_2, the observation interval starts at time t_1 till time $t_1 + 6hours$.
In that way, the observation interval is perfectly synchronized with the fault and each detection can be accurately evaluated during the analysis.

6.2.1 Compression Artifacts - Spikes and Losses

The results reported in this subsection, are relative to 5 different failure scenarios affecting the CGM signal: scenario 1 corresponds to the presence of a spike, scenario 2 to the presence of a 10 minutes loss, scenario 3 to the presence of a 20 minutes loss, scenario 4 to the presence of a 30 minutes loss, scenario 5 to the presence of a 60 minutes loss.
For each scenario, different amplitudes of these failures were considered: $A = -7.5, -10, -15, -20, -25mg/dl$. Moreover, has always been first tested the algorithm on clean data (without any faults), thus identify the amount of false alarms due to noise.
For each scenario, it is shown a Figure in which the method is applied on a representative patient, taken to the pool of the 100 simulated. The fault amplitude used in each case is was $-25mg/dl$. It's to note that in all the following Figures the glucose signal is re-scaled to the basal, imposed to $120mg/dl$.
In the Figures 6.4, 6.5, 6.6, 6.7, 6.8:

- the blue bars are the True Negative (TN);
- the red bars are the False Negative (FN);
- the yellow bars are the False Positive (FP);
- the green bars are the True Positive (TP);

The summary of the results, mainly in terms of TP, FP, TN, FN, Sensitivity and Specifcity, on the whole simulated population is reported in the Tables 6.5, 6.6, 6.7, 6.8, 6.9.

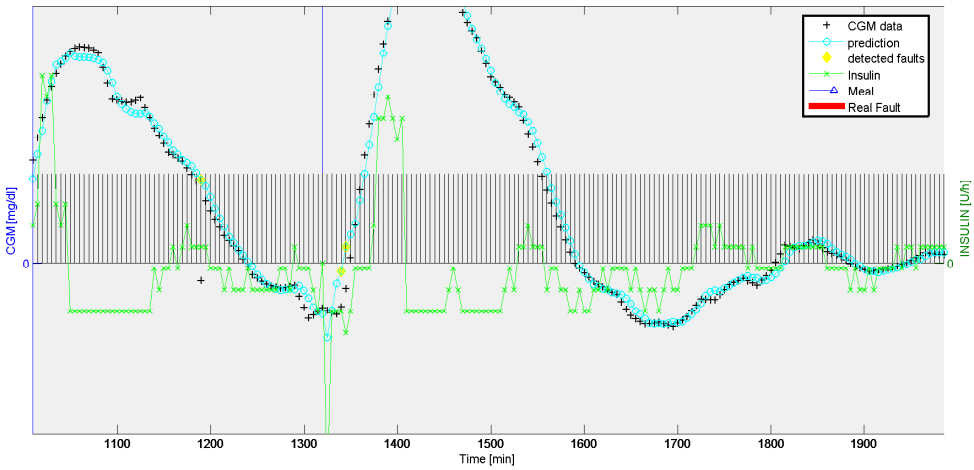

Figure 6.4: Spike at t=1195 min correctly detected by the FDM.

$A =$	0	-7.5	-10	-15	-20	-25
True Negative	28111.00	28100.00	28091.00	28121.00	28100.00	28200.00
False Negative	0.00	38.00	16.00	13.00	15.00	14.00
False Positive	620.00	644.00	647.00	616.00	634.00	609.00
True Positive	0.00	62.00	84.00	87.00	85.00	86.00
PPV [%]	0.00	8.78	11.49	12.38	11.82	12.37
NPV [%]	100.00	99.86	99.94	99.95	99.95	99.95
Sensitivity [%]	NaN	62.00	84.00	87.00	85.00	86.00
Specificity [%]	97.79	97.76	97.75	97.86	97.79	97.89
Accuracy [%]	97.79	97.64	97.70	97.82	97.75	97.84
N EVENTS	0	100.00	100.00	100.00	100.00	100.00

Table 6.5: Result analysis on Scenario 1 - CGM spike.

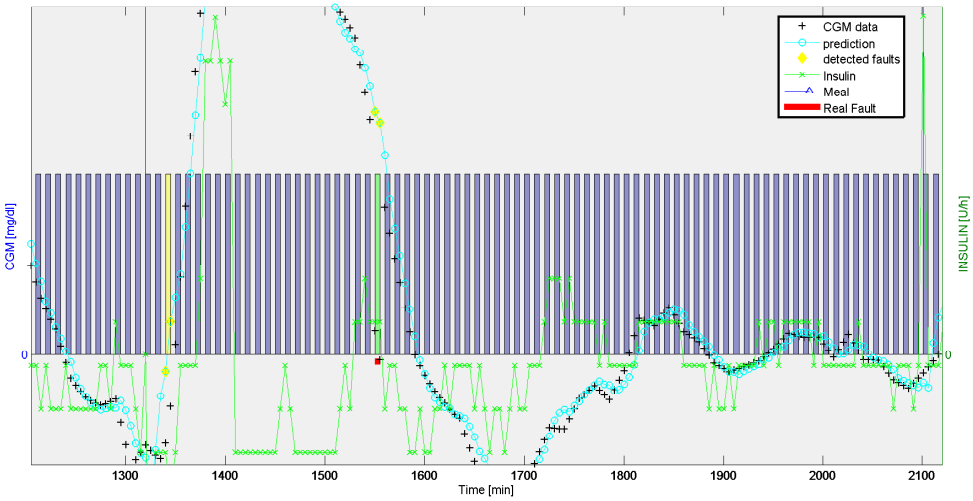

Figure 6.5: 10 minutes of CGM loss of sensitivity, correctly detected by the FDM.

	$D = 0$	$D = 10$ min				
$A =$	0	-7.5	-10	-15	-20	-25
TN	56783	18560	18559	18541	18559	18555
FN	0.00	36.00	14.00	10.00	11.00	9.00
FP	917.00	543.00	535.00	528.00	535.00	533.00
TP	0.00	63.00	85.00	90.00	89.00	91.00
PPV	0.00	10.40	13.71	14.56	14.26	14.58
NPV	100.00	99.81	99.92	99.95	99.94	99.95
Sensitivity [%]	NaN	63.64	85.86	90.00	89.00	91.00
Specificity [%]	98.41	97.16	97.20	97.23	97.20	97.21
Accuracy [%]	98.41	96.98	97.14	97.19	97.16	97.18
N EVENTS	0.00	99.00	99.00	100.00	100.00	100.00

Table 6.6: Result analysis on Scenario 2 - CGM 10 minutes loss of sensitivity.

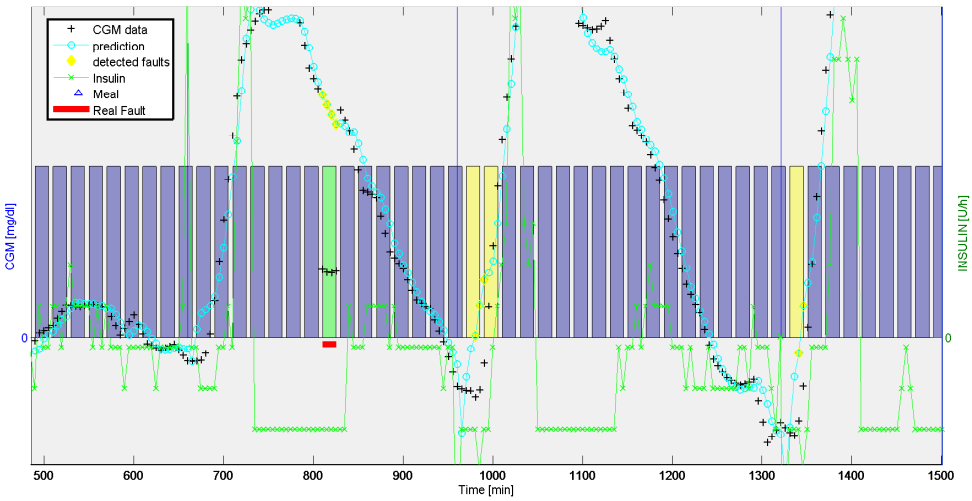

Figure 6.6: 20 minutes of CGM loss of sensitivity, correctly detected by the FDM.

	$D = 20$ min				
$A =$	-7.5	-10	-15	-20	-25
TN	10925	10947	10923	10989	10967
FN	34.00	13.00	3.00	7.00	7.00
FP	456.00	449.00	446.00	430.00	426.00
TP	66.00	87.00	97.00	93.00	93.00
PPV	12.64	16.23	17.86	17.78	17.92
NPV	99.69	99.88	99.97	99.94	99.94
Sensitivity [%]	66.00	87.00	97.00	93.00	93.00
Specificity [%]	95.99	96.06	96.08	96.23	96.26
Accuracy [%]	95.73	95.98	96.09	96.21	96.23
N EVENTS	100.00	100.00	100.00	100.00	100.00

Table 6.7: Result analysis on Scenario 3 - CGM 20 minutes loss of sensitivity.

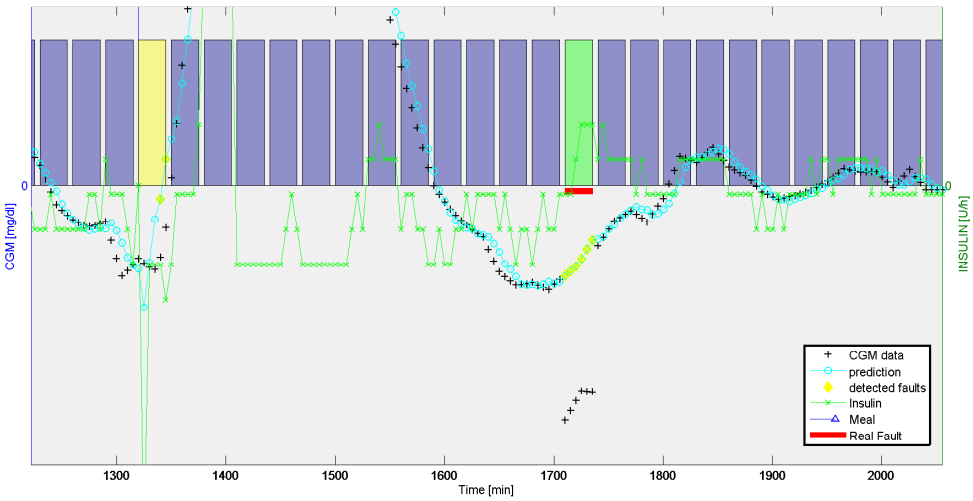

Figure 6.7: 30 minutes of CGM loss of sensitivity, correctly detected by the FDM.

	$D = 30$ min				
$A =$	-7.5	-10	-15	-20	-25
TN	7676	7693	7724	7748	7739
FN	29.00	19.00	7.00	4.00	7.00
FP	409.00	406.00	399.00	375.00	391.00
TP	71.00	81.00	93.00	96.00	93.00
PPV	14.79	16.63	18.90	20.38	19.21
NPV	99.62	99.75	99.91	99.95	99.91
Sensitivity [%]	71.00	81.00	93.00	96.00	93.00
Specificity [%]	94.94	94.99	95.09	95.38	95.19
Accuracy [%]	94.65	94.82	95.06	95.39	95.16
N EVENTS	100.00	100.00	100.00	100.00	100.00

Table 6.8: Result analysis on Scenario 4 - CGM 30 minutes loss of sensitivity.

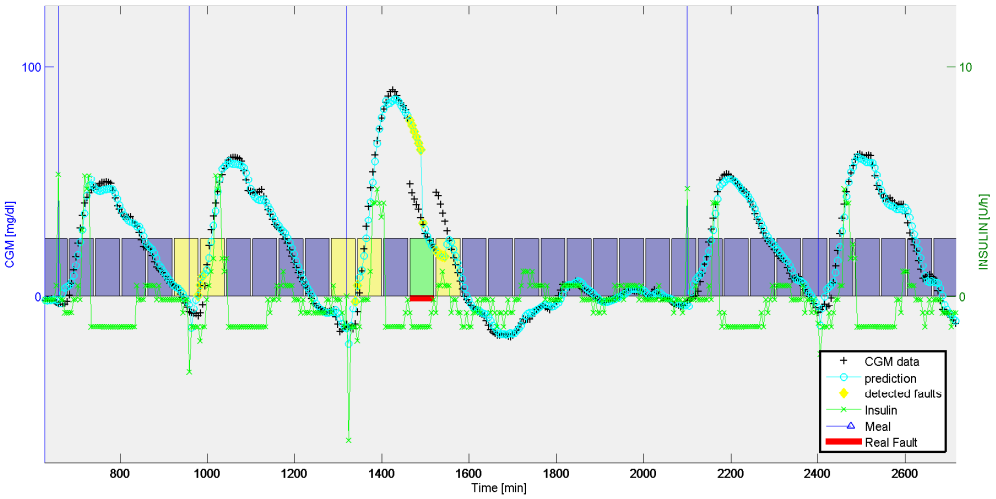

Figure 6.8: 1 hour of CGM loss of sensitivity, correctly detected by the FDM.

	$D = 60$ min				
$A =$	-7.5	-10	-15	-20	-25
TN	3968	3946	3923	3914	3902
FN	32.00	17.00	8.00	15.00	6.00
FP	354.00	370.00	410.00	418.00	414.00
TP	68.00	83.00	92.00	85.00	94.00
PPV	16.11	18.32	18.33	16.90	18.50
NPV	99.20	99.57	99.80	99.62	99.85
Sensitivity [%]	68.00	83.00	92.00	85.00	94.00
Specificity [%]	91.81	91.43	90.54	90.35	90.41
Accuracy [%]	91.27	91.24	90.57	90.23	90.49
N EVENTS	100.00	100.00	100.00	100.00	100.00

Table 6.9: Result analysis on Scenario 5 - CGM 1 hour loss of sensitivity.

As visible from these results, the performance of this method in detecting of the compression artifacts are really positive.
In Figure 6.4, the spike appears at $t = 1195min$ and it can be seen how in this case the fault it's well detected by the algorithm. The prediction is quite different from the measurement that arrived, so the method directly compering these two informations, correctly alarm on the presence of the spike.
Focusing on the entire scenario 1, Table 6.5 shows how the specificity is always very high, over 97%. Moreover the sensitivity is about 85% for each spike amplitude excluding the case of $7.5mg/dl$, in which the spike is small and can be confused with the noise on this signal. These two results evidence that the method identifies hardly as a spike a sample that is not (a few FP), as well as are limited the cases in which the spikes are confused with the CGM noise and dynamic (a few FN). While in all the other cases it detects the spikes correctly when they occur.
Considering now the losses the situation improves even more.
Figures 6.5 and 6.6, show two small losses respectively of 10 and 20 minutes. The first one starts at $t = 1555min$ and ends at $t = 1560min$, while the second one starts at $t = 815min$ and ends at $t = 830min$.
In both the cases can be seen how the predictions are clearly different from the measurements, and also how the latter are not consistent with the CGM dynamics and the inputs nearby. Also these two faults are correctly detected by the method.
Figure 6.7, shows a longer loss of 30 minutes that starts at $t = 1715min$ and ends at $t = 1740min$, perfectly detected.
Finally in Figure 6.8, it is shown the longest simulated loss (1 hour). It starts at $t = 1470min$ and ends at $t = 1525min$. The algorithm detected the fault very quickly, and can be seen how it proceeds with its predictions for 6 steps and than it turns off. Thus, it is re-initialized, and again it detects that something is wrong because the new starting point is on the final phase of the loss. After others 6 samples, it turn off again and finally it is rightly re-initialized.
In all the cases reported on the Tables 6.6, 6.7, 6.8 and 6.9, the specificity wanders on percentages of about 95%, in some cases even 97%. In addition the sensitivity remains high for all the amplitudes and durations. The fact that for a period of 60 minutes the latter decreases to about 91% is due to the fact that the observation interval it's rather large (12 samples), thus the weight of the FP in the final results is more relevant.

Actually the presence of FP, i.e. samples that are not faulty but are recognized as faulty by the algorithm, is an issue that can not be hidden and which must be enhanced in the future. However, it must also keep in mind that the ultimate analysis were done without interruption (night and day) for 2.5 days, for each subject. Comparing these results with those relative to night-only scenario obtained in the article of *Facchinetti et al.* [1], it can be seen that performances are essentially comparable. It can be concluded, therefore, that the prediction and the alarm strategy implemented in relation to compression artifacts, were found to be adequate for the detection and satisfactory.

6.2.2 Meal and Meal-Bolus Failures

In this subsection are reported the results concerning 4 different failure scenarios, relative to the meal event: scenario 1 and scenario 2 involving respectively, the percentage decrease and the percentage increase of the meal amount, while scenario 3 and 4 are respectively about the percentage decrease and the percentage increase of the insulin bolus due to meal event.
For each scenario, the following fault percentages were considered: $E = -100\%$, $-75\%, -50\%, -25\%, +25\%, +50\%, +75\%, +100\%$. As in the previous cases, it has been tested the algorithm on clean data to identify the amount of false alarms due to noise.
For each scenario two Figures of a representative patient are shown. The fault amplitudes used in each case were $-100\%, -50\%$ and $+50\%, +100\%$.
The meaning of the bars in Figures 6.9, 6.10, 6.11 and 6.12 is the same of the previous Figures and the summery of the results, mainly in terms of TP, FP, TN, FN, Sensitivity and Specifcity, on the whole simulated population is reported in the Tables 6.10, 6.11, 6.12, 6.13.

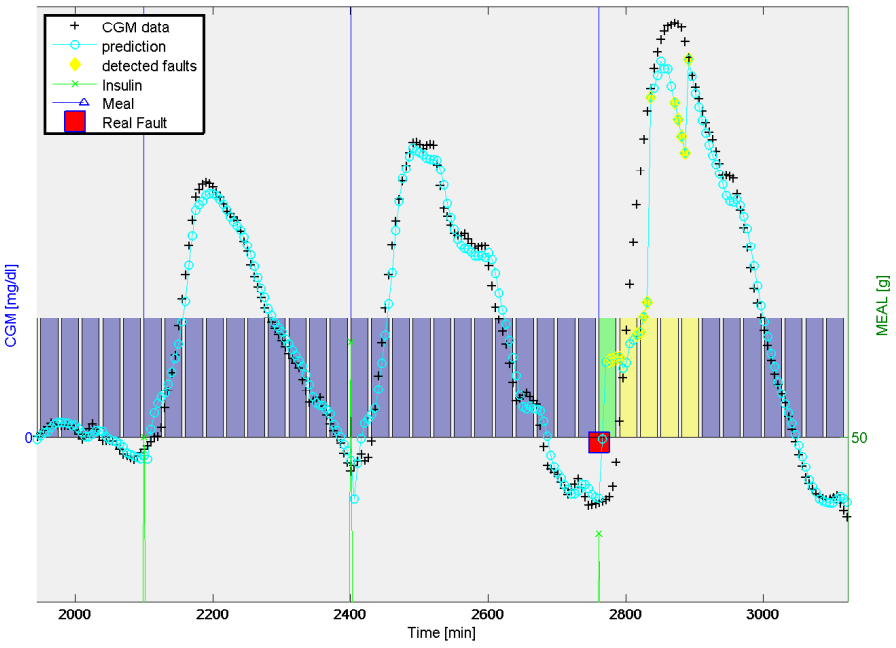

(a) The dinner announcement was reduced by 50%

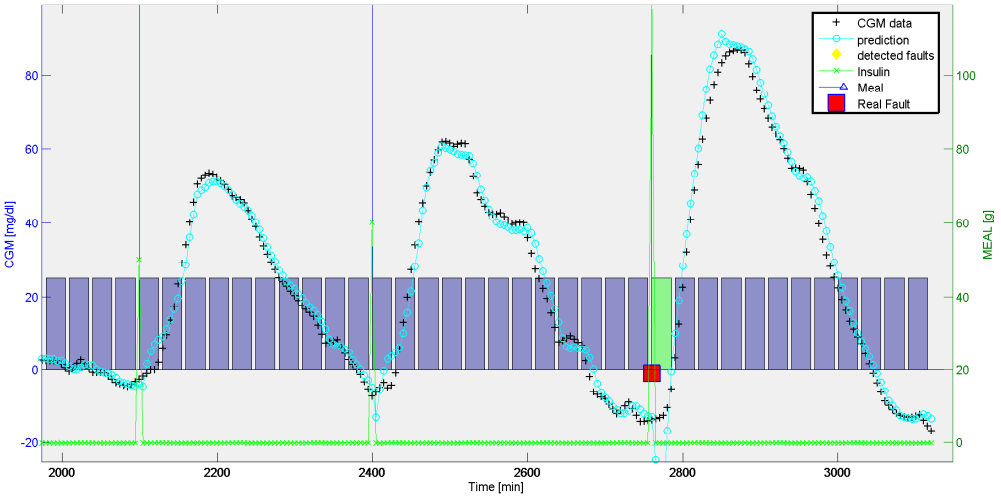

(b) The dinner announcement was reduced by 100%

Figure 6.9: 50% (a) and 100% (b) decrease of the meal amplitude announcement, correctly detected by the FDM.

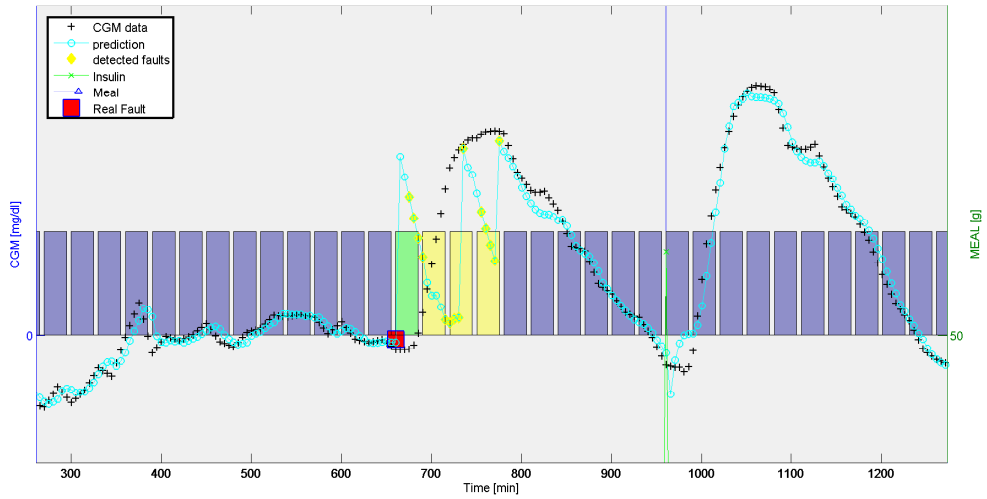

(a) The breakfast announcement was increased by 50%

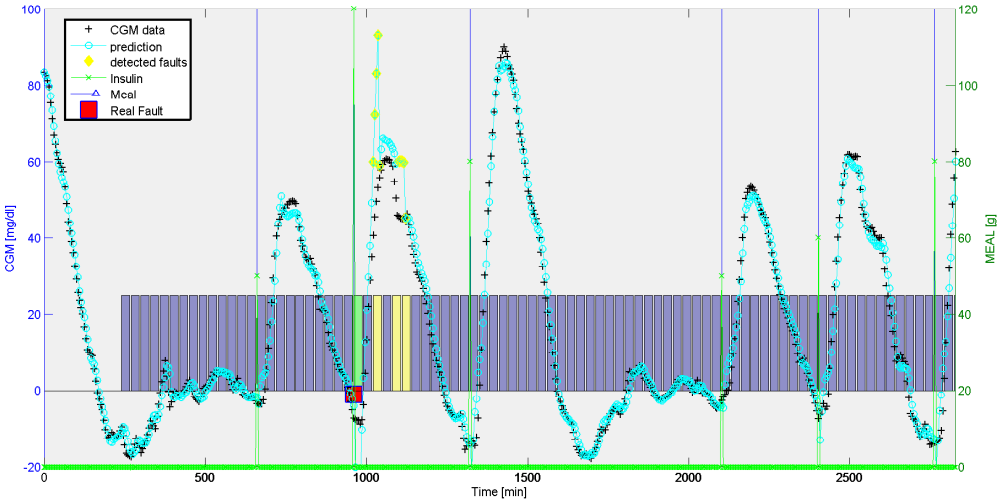

(b) The lunch announcement was increased by 100%

Figure 6.10: 50% (a) and 100% (b) increase of the meal amplitude announcement, correctly detected by the FDM.

$E =$	-100 %	-75 %	-50 %	-25 %	0 %
True Negative	906.00	906.00	910.00	903.00	977.00
False Negative	0.00	0.00	1.00	15.00	0.00
False Positive	194.00	194.00	190.00	197.00	223.00
True Positive	100.00	100.00	99.00	85.00	0.00
PPV [%]	34.01	34.01	34.26	30.14	0.00
NPV [%]	100.00	100.00	99.89	98.37	100.00
Sensitivity [%]	100.00	100.00	99.00	85.00	NaN
Specificity [%]	82.36	82.36	82.73	82.09	81.42
Accuracy [%]	83.83	83.83	84.08	82.33	81.42
N EVENTS	100.00	100.00	100.00	100.00	0

Table 6.10: Result Analysis on Scenario 1 - decrease of the meal amplitude announcement.

$E =$	+25 %	+50 %	+75 %	+100 %
True Negative	917.00	925.00	912.00	932.00
False Negative	47.00	11.00	5.00	2.00
False Positive	183.00	175.00	188.00	168.00
True Positive	53.00	89.00	95.00	98.00
PPV [%]	22.46	33.71	33.57	36.84
NPV [%]	95.12	98.82	99.45	99.79
Sensitivity [%]	53.00	89.00	95.00	98.00
Specificity [%]	83.36	84.09	82.91	84.73
Accuracy [%]	80.83	84.50	83.92	85.83
N EVENTS	100.00	100.00	100.00	100.00

Table 6.11: Result Analysis on Scenario 2 - increase of the meal amplitude announcement.

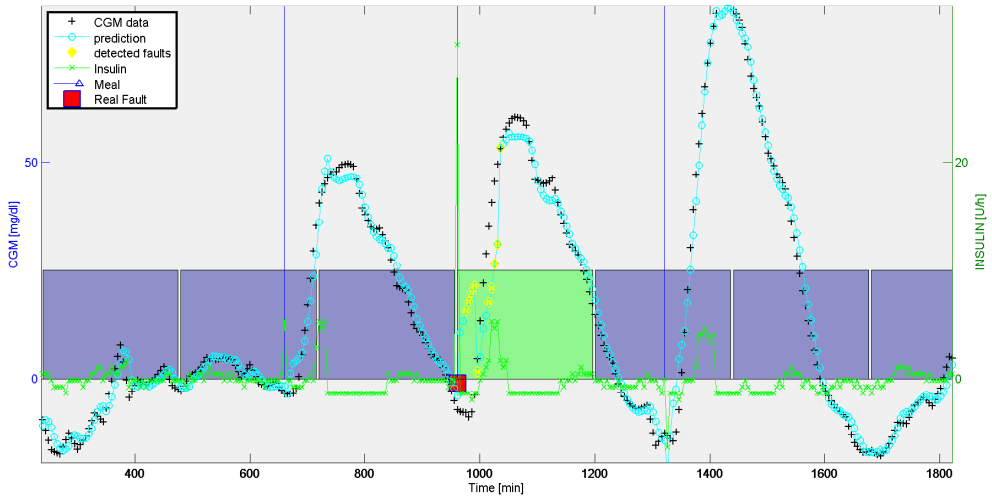

(a) The insulin bolus of the lunch was reduced by 50%

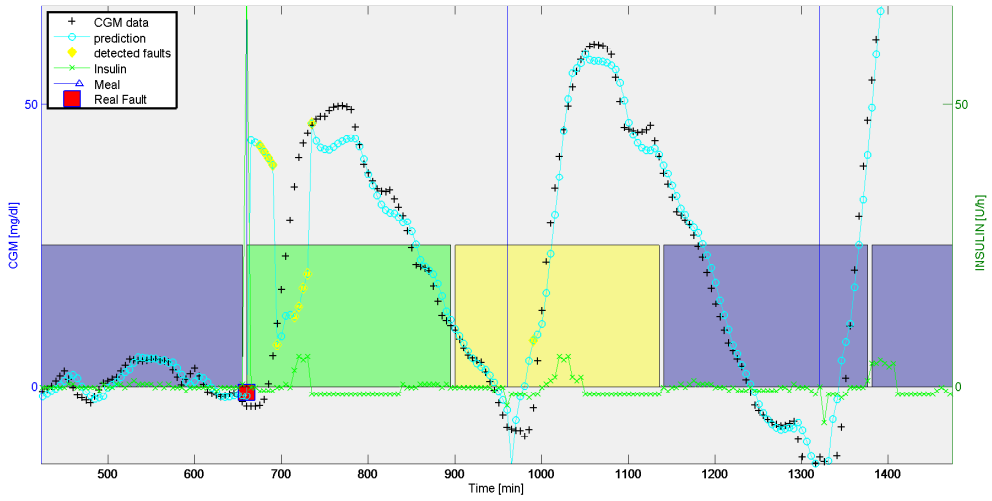

(b) The insulin bolus of the breakfast was reduced by 100%

Figure 6.11: 50% (a) and 100% (b) decrease of the meal-bolus amplitude, correctly detected by the FDM.

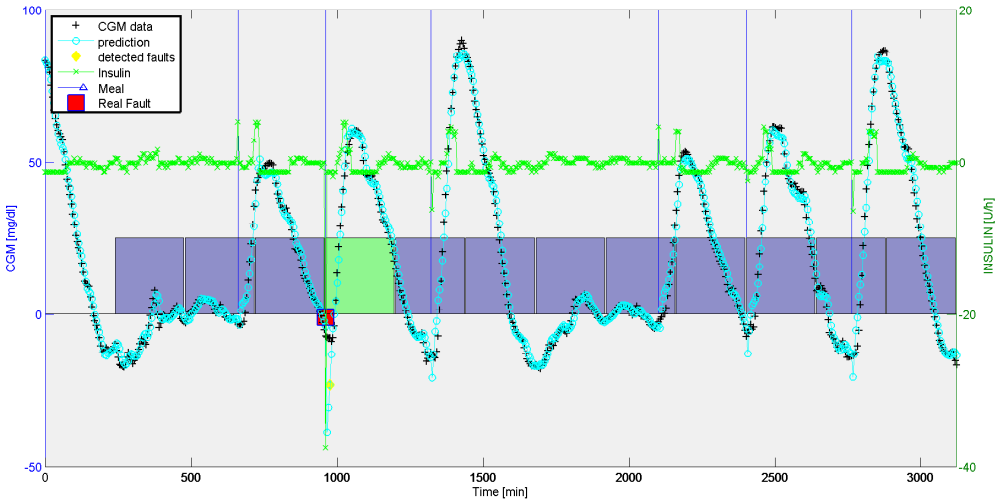

(a) The insulin bolus of the lunch was increased by 50%

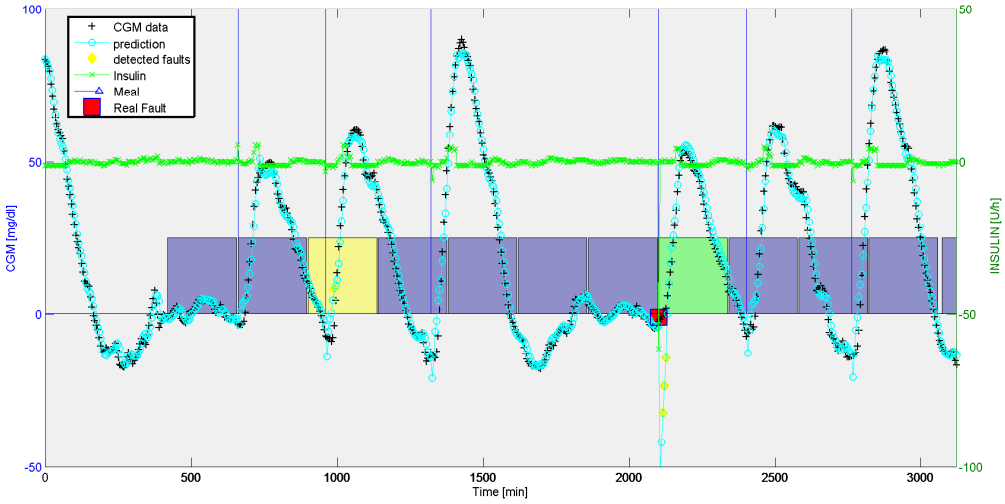

(b) The insulin bolus of the breakfast was increased by 100%

Figure 6.12: 50% (a) and 100% (b) increase of the meal-bolus amplitude, correctly detected by the FDM.

$E =$	-100 %	-75 %	-50 %	-25 %	0 %
True Negative	917.00	919.00	908.00	922.00	977.00
False Negative	5.00	7.00	22.00	47.00	0.00
False Positive	183.00	181.00	192.00	178.00	223.00
True Positive	95.00	93.00	78.00	53.00	0.00
PPV [%]	34.17	33.94	28.89	22.94	0.00
NPV [%]	99.46	99.24	97.63	95.15	100.00
Sensitivity [%]	95.00	93.00	78.00	53.00	NaN
Specificity [%]	83.36	83.55	82.55	83.82	81.42
Accuracy [%]	84.33	84.33	82.17	81.25	81.42
N EVENTS	100.00	100.00	100.00	100.00	0

Table 6.12: Result Analysis on Scenario 3 - decrease of the meal-bolus amplitude.

$E =$	+25 %	+50 %	+75 %	+100 %
True Negative	904.00	904.00	928.00	931.00
False Negative	20.00	7.00	3.00	3.00
False Positive	196.00	196.00	172.00	169.00
True Positive	80.00	93.00	97.00	97.00
PPV [%]	28.99	32.18	36.06	36.47
NPV [%]	97.84	99.23	99.68	99.68
Sensitivity [%]	80.00	93.00	97.00	97.00
Specificity [%]	82.18	82.18	84.36	84.64
Accuracy [%]	82.00	83.08	85.42	85.67
N EVENTS	100.00	100.00	100.00	100.00

Table 6.13: Result Analysis on Scenario 4 - increase of the meal-bolus amplitude.

Both the meal failures and the meal-bolus failures, gave very satisfactory outcomes. In Figure 6.9 (a) and (b), the meals that suffered the decrease are the dinners, both well identify by the algorithm. The method worms satisfactorly also in both cases of Figure 6.10 (a) and (b) of scenario 2, where the meals that suffered the increase are the breakfast and the lunch.
It can be seen also by these Figures that, after the detection of the fail as TP, some FP appear as result of the algorithm necessity of assessment after the failure.

In Figure 6.11 (a) and (b), the insulin bolus that suffered the decrease are respectively, the lunch and the breakfast like the two showed in Figure 6.12 (a) and (b) of scenario 2, where the bolus-meal values were increased. In all these simulated

situations, the algorithm detected in a really positive way all the faults.

The considerations on the results can certainly start from the sensitivity row of the Tables 6.11, 6.10, regarding the meal faults. In fact, the method is able to correctly identify these failures in the 90% of the cases when the amplitude of the meal in modulus is equal $|E| \geq 50\%$. In particular, if the amplitude is strictly greater than 50%, $|E| > 50\%$, the failures are correctly detected in the 95% of the cases.
With regard at the sensitivity, in Tables 6.13 and 6.12, it can be seen that the preformance in case of meal-bolus faults are slightly worse, but generally positive and satisfactory. In fact when the amplitude is strictly greater than 50% the failures are correctly detected in the 93% of the cases and, when lower, the percentage falls to 80%.
Therefore, this new method is effective in detecting these kind of faults and at the same time its specificity is good. Looking at the specificity row of the all the 4 previous Tables, for all the amplitude that were considered. This percentage is always grater than 80% and this is an effect of the limited number of False Positive generated.
Note that it would have been possible increasing the performances in terms of correct detection (TP), but this would have increased the number of FP.
Here a conservative and robust implementation was chosen, focused on reducing the numbers of false alarms. Finally, another proof of the robustness of this method in detecting these two kind of failures, are the accuracy values. As it can be seen from the Tables below, it is always higher than 80%, a suitable percentage in correctly classifying a sample.

6.2.3 Basal Failures

The last fault studied, is the insulin basal failure.
In Figure 6.13, 6.14 and 6.15 it can be seen the result of the detection in one representative subject, in all the simulated scenarios that involve this kind of failure: its duration in scenario 1 is 1 hour, in scenario 2 is 2 hours, in scenario 3 is 3 hours, in scenario 4 is 4 hours, in scenario 5 is 6 hours.
For each scenario, the following fault percentages were considered: $E = -100\%$, $-75\%, -50\%, -25\%, +25\%, +50\%, +75\%, +100\%$ and as usual the algorithm has been tested on clean data to identify the amount of false alarms due to noise.
In the following Figures the fault amplitudes reported are $-100\%, -50\%$ and $+50\%, +100\%$.
The meaning of the bars is still the same given in the previous subsection and the summary of the results, mainly in terms of TP, FP, TN, FN, Sensitivity and Specifcity, on the whole simulated population is reported in the Tables 6.14, 6.15, 6.16, 6.17, 6.18.

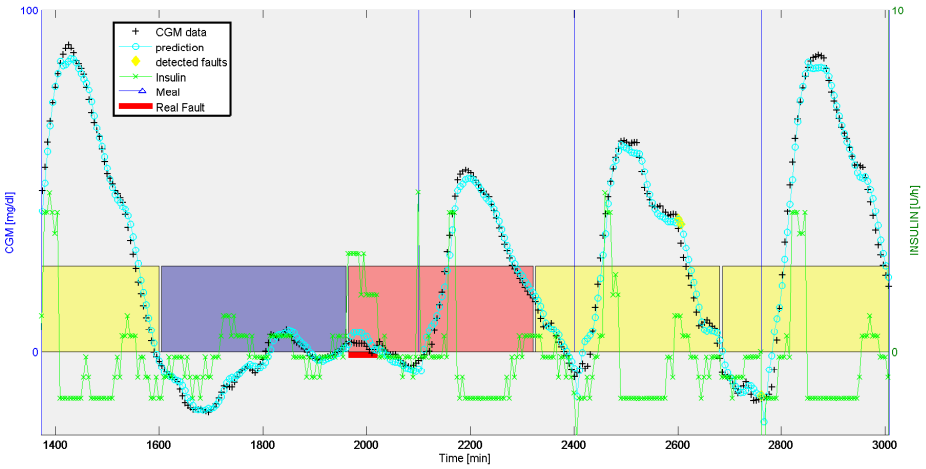

Figure 6.13: 1 hour basal failure starts at t=1970 min. The FDM was unable to detect it.

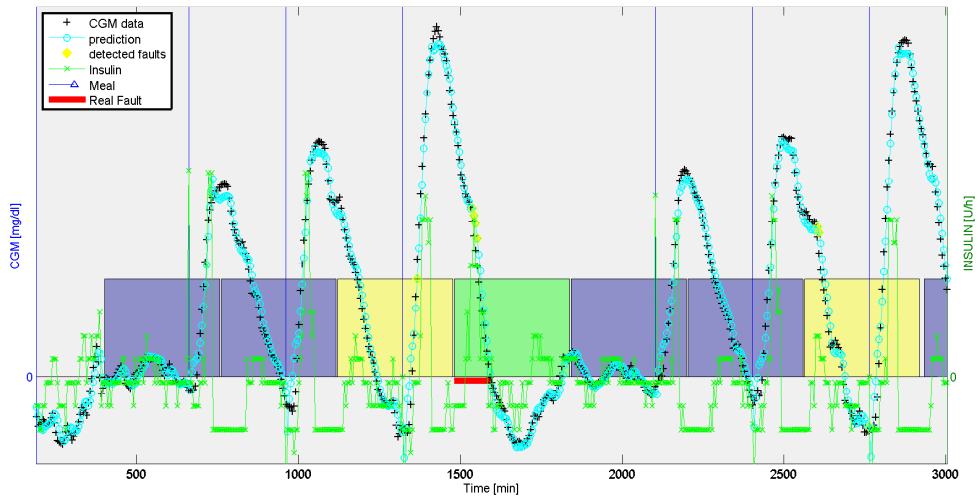

(a) The 2 hours of basal failure were detected by the FDM.

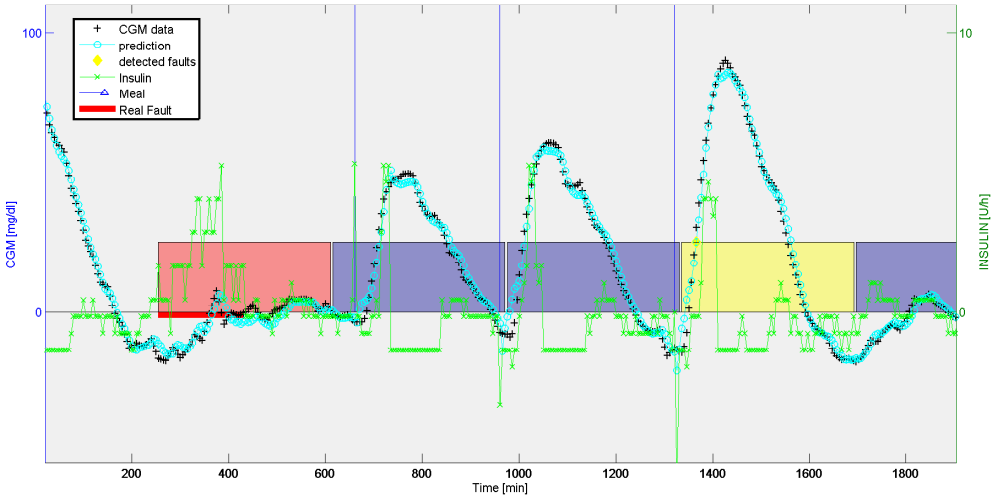

(b) The 3 hours of basal failure were not detected by the FDM.

Figure 6.14: In (a) occur 2 hours of basal failure; in (b) occur 3 hours of basal failure.

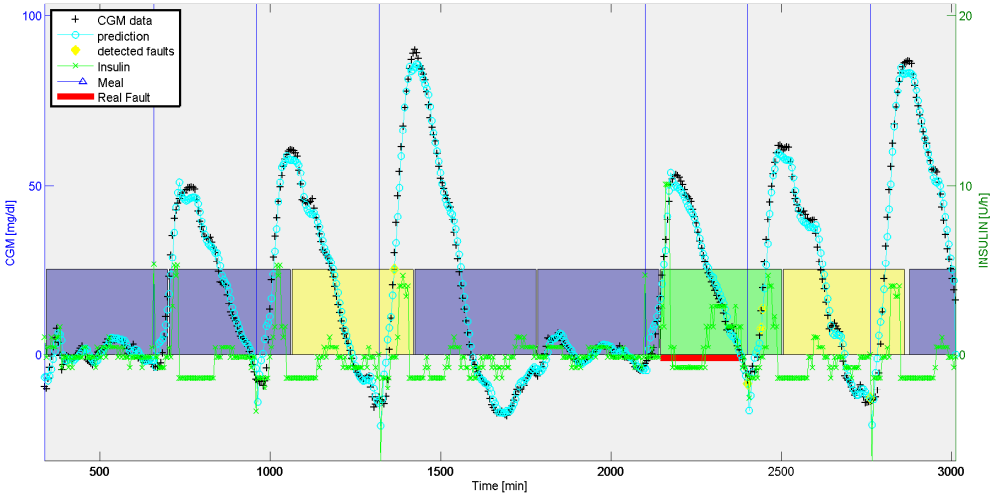

(a) The 4 hours of basal failure were detected by the FDM.

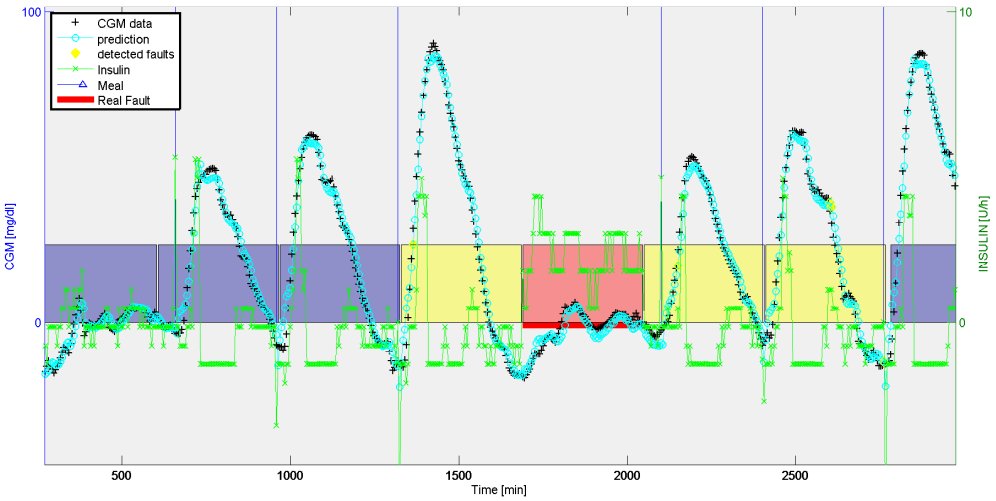

(b) The 6 hours of basal failure were not detected by the FDM.

Figure 6.15: In (a) occur 4 hours of basal failure; in (b) occur 6 hours of basal failure.

	$D = 1$ hour				
$A =$	-100 %	-50 %	0 %	50 %	100%
TN	597.00	601.00	684.00	603.00	592.00
FN	82.00	79.00	0.00	82.00	87.00
FP	33.00	29.00	30.00	32.00	30.00
TP	18.00	21.00	0.00	18.00	13.00
PPV	14.88	18.10	0.00	15.65	10.92
NPV	87.92	88.38	100.00	88.03	87.19
Sensitivity [%]	18.00	21.00	NaN	18.00	13.00
Specificity [%]	94.76	95.39	95.79	94.96	95.17
Accuracy [%]	84.25	85.21	95.80	84.49	83.80
N EVENTS	100.00	100.00	0.00	100.00	100.00

Table 6.14: Result Analysis on Scenario 1 - 1 hour with basal amplitude reduction of 50%.

	$D = 2$ hour				
$A =$	-100 %	-50 %	0 %	50 %	100%
TN	590.00	595.00	684.00	599.00	596.00
FN	73.00	84.00	0.00	87.00	84.00
FP	30.00	31.00	28.00	30.00	31.00
TP	27.00	16.00	0.00	13.00	16.00
PPV	19.85	13.33	0.00	11.40	13.45
NPV	88.99	87.63	100.00	87.32	87.65
Sensitivity [%]	27.00	16.00	NaN	13.00	16.00
Specificity [%]	95.16	95.04	96.06	95.23	95.05
Accuracy [%]	85.69	84.16	96.07	83.95	84.18
N EVENTS	100.00	100.00	0.00	100.00	100.00

Table 6.15: Result Analysis on Scenario 2 - 2 hours with basal amplitude reduction of 50%.

	$D = 3$ hours				
$A =$	-100 %	-50 %	0 %	50 %	100%
TN	592.00	597.00	684.00	585.00	593.00
FN	60.00	79.00	0.00	69.00	63.00
FP	31.00	28.00	0.00	33.00	30.00
TP	40.00	21.00	0.00	31.00	37.00
PPV	21.32	16.67	0.00	8.73	17.32
NPV	89.29	88.18	100.00	86.80	88.38
Sensitivity [%]	29.00	20.00	NaN	11.00	22.00
Specificity [%]	84.69	85.65	85.50	83.57	84.96
Accuracy [%]	77.72	77.42	85.50	74.50	77.07
N EVENTS	100.00	100.00	0.00	100.00	100.00

Table 6.16: Result Analysis on Scenario 3 - 3 hours with basal amplitude reduction of 50%.

	$D = 4$ hours				
$A =$	-100 %	-50 %	0 %	50 %	100%
TN	590.00	602.00	684.00	592.00	591.00
FN	43.00	63.00	0.00	65.00	48.00
FP	29.00	29.00	0.00	31.00	31.00
TP	57.00	37.00	0.00	35.00	52.00
PPV	23.40	21.77	0.00	17.97	20.44
NPV	89.80	89.19	100.00	88.49	89.14
Sensitivity [%]	33.00	27.00	NaN	23.00	28.00
Specificity [%]	84.53	86.12	85.50	84.94	84.43
Accuracy [%]	78.07	78.72	85.50	77.16	77.38
N EVENTS	100.00	100.00	0.00	100.00	100.00

Table 6.17: Result Analysis on Scenario 4 - 4 hours with basal amplitude reduction of 50%.

	$D = 6$ hours				
$A =$	-100 %	-50 %	0 %	50 %	100%
TN	567.00	583.00	684.00	583.00	571.00
FN	68.00	85.00	0.00	84.00	75.00
FP	132.00	115.00	116.00	116.00	127.00
TP	32.00	15.00	0.00	16.00	25.00
PPV	19.51	11.54	0.00	12.12	16.45
NPV	89.29	87.28	100.00	87.41	88.39
Sensitivity [%]	32.00	15.00	NaN	16.00	25.00
Specificity [%]	81.12	83.52	85.50	83.40	81.81
Accuracy [%]	74.97	74.94	85.50	74.97	74.69
N EVENTS	100.00	100.00	0.00	100.00	100.00

Table 6.18: Result Analysis on Scenario 5 - 6 hours with basal amplitude reduction of 50%.

In Figure 6.13, the basal failure starts at $1970min$ and lasts 1 hour till $2025min$. The algorithm doesn't succeed in the identification of the fault and also causes 3 false alarms. In Figure 6.14 (a) and 6.15 (a), the duration of the fault is longest, respectively 2 and 4 hours, and the algorithm detects them, but it also generates two FP.

In the other two cases rapresented in Figure 6.14 (b) and 6.15 (b), the method fails to detect the faults; moreover it still generates false alarms.

As already mentioned above, this is certainly the most challenging scenario because of the difficulties due to the identification of suitable models which succeed in predicting the glycemia for many steps ahead. The latter are undoubtedly needed to success in take into account the effect of some basal perturbations on the CGM traces.

It is for this reason, with a reasoning similar to that used for the other failures, that the strategy used to alarm should be robust and conservative, i. e. it is preferable to detect only in few cases the fault (low TP) and not to generate a lot of FP.

Considering the Tables 6.14, 6.15, 6.16, 6.17 and 6.18 and looking at Sensitivity row, it can be seen how the strategy developed for the detection, doesn't work as satisfactory as in the previous scenarios. The algorithm detected the fault only the 20% of the times. As anticipated, the problem could stay in the identification of an inadegaute model for such a scope.

On the other hand, adapting the method developed with the third alarm strategy

described in the previous chapter, the percentages of the specificity are about 90%: so also this time the number of False Positive is controlled.

Chapter 7

Future Developments

The way ahead for the development of a robust fault detection method is still long, but the job that was done in the last year, lays the foundation for important improvements.
The results presented in this thesis demonstrated that the FDM results very effective with all the failures associated with the CGM sensor and with the meal event, expecially in what concerns them detection. The latter was also very positive regarding the basal failures.
Focusing on the results concerning the false alarm that were obtained, the method is able to contain them under the 20% with the exception of the basal fault that, as was largely discussed during the thesis, still need some improvements especially on the model identification. This result is much perspective, considering both the data set used, which presented a large variability inter-individual, and the continue detection for 2.5 full days.
It will start now, a study on the development of the FDM using real data.
The method will be re-adapted for this new challenge, because the real data are more difficult to analyze than those simulated and present some new problems.
Once that will be obtained satisfactory and safe results on real data, the next step will be the development a new module of Fault Detection on the Artificial Pancreas, that will ensure greater patient safety and with contemporary improvements of all the other parts and modules of the system, it will provide an utilization of the AP as an alternative to traditional therapy for the treatment of diabetes millitus Type I.

Chapter 8

Appendix A

8.1 Initialization of the DiAs

The DiAs can operate in two modes called **open loop** and **colsed loop**. Both to be activated, need some informations that must be entered by the team work concerning:

- Some generical subject information (see Figure 8.1(a));
- The Correction Factor profile that consists of a series of time entered each of which is associated with a value for the correction factor in $mg/dl/U$ (see Figure 8.1(b));
- The Carbohydrate to Insulin Ratio profile that consists of a series of segments entered each of which is associated with a value for the carbohydrate to insulin ratio in g/U (see Figure 8.1(c));
- The Basal profile consists of a series of segments entered each of which is associated with a value for the basal insulin delivery rate in $U/hour$ (see Figure 8.1(d));

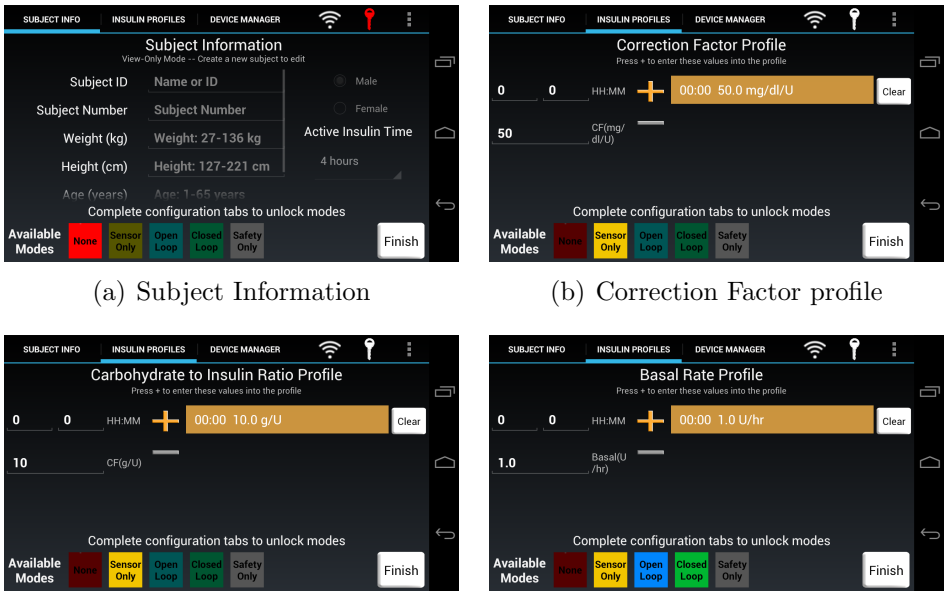

(a) Subject Information

(b) Correction Factor profile

(c) Carbohydrate to Insulin Ratio profile

(d) Basal profile

Figure 8.1: DiAs Initialization.

8.2 Open Loop Mode

The open loop therapy is the same one taken normally by the patient. The only difference is that the DiAs controls the pump, with which the basal insulin (setted in the *Basal Profile* tab), the meal bolus and if necessary some correction bolus requested by the patient, are delivered.
Futhermore the DiAs, being also connected to the CGM system, displays at the center of the screen the last CGM measurement like the CGM reciver.
During the course of the open loop, the patient has to insert a few informations such as, before the meal, the amount of carbohydrates that will be eaten or, if happen, eventually hypo-treatment.
This mode is useful to compere the standard therapy with the colsed loop therapy and so to try to understand how and where the system must be improved and when it works better than the standard therapy.
The main screen of the DiAs during the Open Loop mode is reported in Figure 8.2.

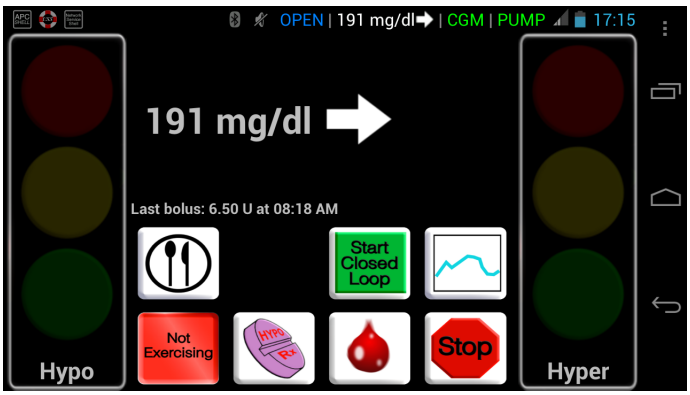

Figure 8.2: DiAs Open Loop Mode.

8.3 Closed Loop Mode

With the closed loop therapy, the algorithms developed for the glycemic control take the command of the entire system.
In all early AP, the closed-loop control algorithms belonged to the class of **p**ropotional-**i**ntegral-**d**erivative, **PID**, controllers which calculated the insulin bolus in a straightforward way. Their utilization was limited in subcutaneous systems because of unavoidable time lags in subcutaneous glucose sensing and insulin action, [11], so another control approach was developed: it is the **m**odel-**p**redictive-**c**ontrol, **MPC**, which avoid the PID limitations by using a mathematical model of the metabolic system of the person being controlled, [11], and that showed a great ability to keep glucose control in a safe near-normal range.
In the closed-loop mode, the DiAs still required some user inputs to inform the control algorithm that a particular event is happening. Usually, this is necessary before meals and whenever the system signaled imminent risk for hypoglycemia or hyperglycemia. To alert about the latter risks, located at either side of the main screen there are two *traffic light* symbols, see Figure 8.3. If the red hypoglycemia light turns on, it indicates that the system believes that this condition is imminent or already underway and an alarm will start to sound. Until now the protocols developed says that in this case, the patient must check his blood sugar and must be treat with about 15g of carbohydrate, $\approx$ 3 sugar sachets, immediately. Otherwise if the lights are green or yellow, the algorithms are properly working.
If instead, the red hyperglycemia light turns on, it indicates that the system believes that this other condition can't be avoided and also in this case a control intervention

is required.

Figure 8.3: DiAs Closed Loop Mode.

In 2010, the European Commission launching the *AP@Home project*, which involves 7 universities and 5 companies throughout Europe, [11]. The project is arriving almost at the end; during the 2013 were concluded all the scheduled outpatient trials in Padova (Italy), Montpellier (France) and Amsterdam (Netherlands) and is being organized right now, the final phase in which the patients will use the AP system during all the day for 3 mounths with the supervision of the work-team, performed in telemedicine.

Confirmed BG Result (mg/dL)	Frequency of BG Measurement	Treatment Guidelines
≥80	Consider repeat SMBG every ~15-30 mins if clinically indicated (e.g. BG rapidly dropping or Hypoglycemia Red Light persists)	No hypoglycemia treatment. Continue protocol.
70-79	Assess fingerstick SMBG glucose measurements approximately every 15 minutes, or more frequently if BG rapidly dropping (e.g. ≥2 mg/dL/min).	Study MD will be notified. Subject may be treated for hypoglycemia if clinically indicated as determined by MD (e.g. significant symptoms, rapid decline in BG). Continue protocol.
51-69	Assess fingerstick SMBG glucose measurements approximately every 15 minutes, or more frequently if BG rapidly dropping (e.g. ≥2 mg/dL/min).	Study MD will be notified and will supervise the following interventions: Subject will be treated with ~16 grams of glucose (preferably glucose tabs or gel/liquid). Retreatment rules: 1) If the glucose level 15 minutes after treatment is <80 mg/dL, the subject may be treated with an additional ~16 grams of glucose.
≤50 without signs of neuroglycopenia or severe hypoglycemia	Confirm (recheck) original value and assess fingerstick SMBG glucose measurements approximately every 5 minutes until glucose >50 mg/dL.	Study will be stopped. Study MD will be notified and will supervise the following interventions. The insulin pump will be removed/disconnected. The patient will be monitored for neuroglycopenia. Subject will be treated with ~16 grams of glucose (preferably glucose tabs or gel/liquid). Retreatment rules: 1) If the glucose level 5 minutes after treatment is <80 mg/dL, the subject may be treated with an additional ~16 grams of glucose; 2) Once the glucose level is ≥80 mg/dL, no additional treatment will be administered for that hypoglycemic event. NOTE: Oral treatment should not be given if signs of neuroglycopenia or severe hypoglycemia symptoms are present. Refer to treatment of neuroglycopenia or severe hypoglycemia.
Signs of neuroglycopenia (e.g. lethargy, disorientation, confusion [disordered processing of information or communication], or inappropriate behavior) or severe hypoglycemic symptoms (i.e. hypoglycemic seizure, loss of consciousness, or inability to properly consume treatment)	Do not delay treatment for fingerstick assessment. Assess fingerstick SMBG glucose measurements approximately every 5 minutes until glucose >50 mg/dL, then approximately every 15 minutes until BG ≥80 mg/dL	Study will be stopped. Study MD will be notified and will supervise the following interventions: The insulin pump will be removed/disconnected. One amp (1 mg) of glucagon intramuscularly. The drug will be reconstituted per package insert/instructions and administered intramuscularly into either an arm or thigh muscle. Glucagon may be repeated as needed every 20 minutes to achieve glucose level ≥80 mg/dL. SMBG measurements will be performed as requested by study MD. Once the subject is able to consume oral treatment, if glucose level is <80 mg/dL, treatment rules above pertaining to oral treatment will be followed until BG ≥80 mg/dL. However, since orange juice and milk ingestion after glucagon can increase the incidence of nausea and vomiting, use glucose liquid, gel or tablets for oral treatments after glucagon administration. The subject's insulin pump will be started after BG ≥80 mg/dL. Subject will be reassessed and treated every 5 minutes as needed.

Figure 8.4: An *AP@HOME* protocol in cases of hypoglycemia

Confirmed BG Result (mg/dL)	Frequency of BG Measurement	Precision Xtra β-Ketone Measurement Rules	β-Ketone Result (mmol/L)	Treatment Guidelines
≥250 and <300	Fingerstick SMBG glucose measurements approximately every hour until SMBG glucoses <250 mg/dL	β-Ketone measurement every hour until SMBG glucose <250 mg/dL and β-Ketone level is <0.6 mmol/L	<0.6	Study MD will be notified and will supervise the following interventions. Additional correction boluses may be administered no more frequently than every 2 hours as needed to achieve SMBG glucose between 80-250 mg/dL and β-Ketone measurement <0.6 mmol/L. The study pump will be assessed and a new insertion may be performed if clinically indicated. If the study pump has to be replaced or removed due to suspected catheter occlusion, an initial correction insulin dose may be injected subcutaneously using an insulin syringe. Use of subcutaneous insulin will impose a 2 hour open loop segment. If clinically indicated, a manual bolus will be given through the system. Subject may consume ad lib glucose-free beverages.
			≥0.6 - ≤1.0	Study MD will be notified and will supervise the following interventions. Additional correction boluses may be administered no more frequently than every 2 hours as needed to achieve SMBG glucose between 80-250 mg/dL and β-Ketone measurement <0.6 mmol/L. The study pump will be assessed and a new insertion may be performed if clinically indicated. If the study pump has to be replaced or removed due to suspected catheter occlusion, an initial correction insulin dose may be injected subcutaneously using an insulin syringe. Use of subcutaneous insulin will impose a 2 hour open loop segment. Subject may consume ad lib glucose-free beverages. If β-ketone level is ≥0.6 mmol/L for >2 hours or symptoms of nausea, vomiting or abdominal pain are present, the study will be stopped. Subject will restart own insulin pump. Subcutaneous insulin may be provided. Study MD will continue to monitor the situation.
			>1.0	Study will be stopped. Subject will restart own insulin pump. Subcutaneous insulin will be provided. Subject may consume ad lib glucose-free beverages. Study MD will continue to monitor and treat the situation until its resolution.
≥300 mg/dL and ≤400 mg/dL	Fingerstick SMBG glucose every 30 min until SMBG glucose <250	β-Ketone measurement every hour until SMBG glucose <250 mg/dL and β-Ketone level is <0.6 mmol/L	<0.6	Study MD will be notified and will supervise the following interventions. Additional correction boluses may be administered no more frequently than every 2 hours as needed to achieve SMBG glucose between 80-250 mg/dL and β-Ketone measurement <0.6 mmol/L. The study pump will be assessed and a new insertion may be performed if clinically indicated. If the study pump has to be replaced or removed due to suspected catheter occlusion, an initial correction insulin dose may be injected subcutaneously using an insulin syringe. Use of subcutaneous insulin will impose a 2 hour open loop segment. Subject may consume ad lib glucose-free beverages. If SMBG glucose remains >300 mg/dL for > 2 hours, the study will be stopped. Subject will restart own insulin pump. Subcutaneous insulin may be provided. Study MD will continue to monitor the situation.
			≥0.6 - ≤1.0	Study MD will be notified and will supervise the following interventions. Additional correction boluses may be administered no more frequently than every 2 hours as needed to achieve SMBG glucose between 80-250 mg/dL and β-Ketone measurement <0.6 mmol/L. The study pump will be assessed and a new insertion may be performed if clinically indicated. If the study pump has to be replaced or removed due to suspected catheter occlusion, an initial correction insulin dose may be injected subcutaneously using an insulin syringe. Use of subcutaneous insulin will impose a 2 hour open loop segment. Subject may consume ad lib glucose-free beverages. If β-ketone level is ≥0.6 mmol/L for >2 hours or SMBG glucose remains >300 mg/dL for >2 hours or symptoms of nausea, vomiting or abdominal pain are present, the study will be stopped. Subject will restart own insulin pump. Subcutaneous insulin may be provided. Study MD will continue to monitor and treat the situation until its resolution.
			>1.0	Study will be stopped. Subject will restart own insulin pump. Subcutaneous insulin will be provided. Subject may consume ad lib glucose-free beverages. Study MD will continue to monitor and treat the situation until its resolution.
>400 mg/dL	Fingerstick SMBG glucose every 30 min until SMBG glucose <250	β-Ketone measurement every hour until SMBG glucose <250 mg/dL and β-Ketone level is <0.6 mmol/L	Any value	Study will be stopped. Subject will restart own insulin pump. Subcutaneous insulin will be provided. Subject may consume ad lib glucose-free beverages. Study MD will continue to monitor and treat the situation until its resolution.

Figure 8.5: An *AP@HOME* protocol in cases of hyperglycemia

Bibliography

[1] Andrea Facchinetti et al. An online failure detection method of the glucose sensor-insulin pump system: Improved overnight safety of type-1 diabetic subjects. *IEEE Trans Biomed Eng*, 60:406–416, 2013.

[2] E. Widmaier et al. *Vander's Human Physiology.* McGraw - Hill, 11th ed edition, 2007.

[3] E. Renard et al. Towards an artificial pancreas at home. *Diabetes & Metabolism*, 37:94–98, 2011.

[4] E. Renard et al. Closed loop developments to improve glucose control at home. *Diabetes Research and Clinical Practice.*, 2013.

[5] K. L. Helton et al. Biomechanics of the sensor-tissue interface. effects of motion, pressure and design on sensor performance and foreign body response. part ii: Examples and application. *Journal of Diabetes Science and Technology.*, 5:647–656, 2011.

[6] Giorgio Picci. *Filtraggio Stocastico e Applicazioni.* Libreria Progetto, 2006.

[7] Greg Welch and Gary Bishop. An introduction to the kalman filter, 2001.

[8] B. De Moor P. Van Overschee. N4sid: Subspace algorithms for the identification of combined deterministic-stochastic systems. *Automatica, Special Issue on Statistical Processing and Control.*, 1992.

[9] C. Dalla Man et al. Fda approved simulator of type 1 diabetes: an in silico substitute for artificial pancreas preclinical studies. *Proceeding of GNB2008.*, 2008.

[10] Tom Fawcett. An introduction to roc analysis. *Elsevier*, 27:861–874, 2005.

[11] C. Cobelli et al. Artificial pancreas past, present, future. *Diabetes.*, 2011.